# Description and interpretation of fault-related sedimentation and controls on shelf-edge deltas: implication on sand transportation to the basin floor in parts of Eastern Niger Del...

**7 authors**, including:

David Anomneze
Moni Pulo Petroleum Development Limited
**10** PUBLICATIONS **5** CITATIONS

SEE PROFILE

Anthony Okoro
Nnamdi Azikiwe University, Awka
**50** PUBLICATIONS **116** CITATIONS

SEE PROFILE

N. E. Ajaegwu
Nnamdi Azikiwe University, Awka
**24** PUBLICATIONS **50** CITATIONS

SEE PROFILE

Okey Akpunonu
Nnamdi Azikiwe University, Awka
**16** PUBLICATIONS **49** CITATIONS

SEE PROFILE

**Some of the authors of this publication are also working on these related projects:**

Project    PhD Project: Taranaki Basin gas hydrates, submarine landslides and fluid flow dynamics View project

Project    My Lab Research Work View project

# Description and interpretation of fault-related sedimentation and controls on shelf-edge deltas: implication on sand transportation to the basin floor in parts of Eastern Niger Delta

## David O. Anomneze, Anthony U. Okoro, Norbert E. Ajaegwu, Eliseus O. Akpunonu, Izuchukwu I. Obiadi, Chibuzo V. Ahaneku, et al.

Springer

Springer

# Description and interpretation of fault-related sedimentation and controls on shelf-edge deltas: implication on sand transportation to the basin floor in parts of Eastern Niger Delta

David O. Anomneze[1,2] · Anthony U. Okoro[1] · Norbert E. Ajaegwu[1] · Eliseus O. Akpunonu[1] · Izuchukwu I. Obiadi[1] · Chibuzo V. Ahaneku[1] · George C. Okeke[1]

## Abstract

An integrated structural and stratigraphic analysis of a regional dataset from Eastern Niger Delta was undertaken with the objective of improving the present understanding of the structural development, seismic reflection geometries and implication on sand transportation and deposition within the shelf-edge and farther into the basin floor. Well log correlations were carried out using third-order sequence stratigraphy. Fault dynamics and evolution was interpreted with the aid of seismic transect sections, growth fault indexes and dip-extracted semblance slices. Lithofacies and paleobathymetric data were utilized to create gross depositional environment maps for the various sequences from inner-shelf to upper slope environment. The fault dynamics and evolution analysis of co-planar faults shows that older co-planar faults are associated with more accommodation space and depocentres than relatively younger faults. Conceptual subsurface models from this study shows that there is an increase in sand thickness in the proximal part of the sequence associated with precursor (older) faults, while towards the distal part, it reduces. There is also a relative decrease in sand thickness in the proximal part of the sequence associated with younger initiated faults, while towards the distal part, it increases in sand thickness. This study shows that at the shelf-edge, the thickest sand is of the lowstand system tract and the possibility of transporting sands into the basin is more associated with younger co-planar faults with small accommodation space at the shelf-edge, while the precursor older faults retain majority of sand deposits within its subsidence/depocentre axis.

Keywords Shelf-edge deltas play · Fault-controlled sedimentation · Seismic stratigraphy · Co-planar fault evolution

## Introduction

The Niger Delta region is one of the world's major hydrocarbon provinces. It is currently the region producing about 2 MMBL/day of crude in Nigeria today with an available large infrastructure system. The exploration of this province has taken place almost exclusively during the past 63 years. Very few shelf-edge deltas have been explored and documented in the Niger Delta Basin, and they all made significant discoveries (Fig. 1: Amenam Kpono, Oso, Yoho, Sonam, Imo River and Asa Fields). There are still potentially larger and poorly imaged targets within the region (Adereti et al. 2012). Prospecting for such targets requires play-based prediction/analogue models that can be applied to augment the interpretation of poorly imaged targets (Anomneze et al. 2015) and potential new locations of hydrocarbon accumulation. The tectonic history of the Niger Delta depocentre is analogous to the depocentre of the Gulf of Mexico. Forty-one per cent of total identified hydrocarbon pay zones in the Gulf of Mexico have been discovered to be from lowstand prograding wedges of shelf-edge deltas (Wood et al. 2003). This prompted the interest to extensively evaluate the shelf-edge deltas in Nigeria considering their sedimentation and fault associations as they have proven to be associated with higher potential for sand and hydrocarbon accumulation in other basins.

The shelf-edge play is completely different from all other hydrocarbon plays because of its unique depositional setting

✉ David O. Anomneze
davanomneze@gmail.com

1 Geological Sciences, Nnamdi Azikiwe University, Awka, Anambra State, Nigeria

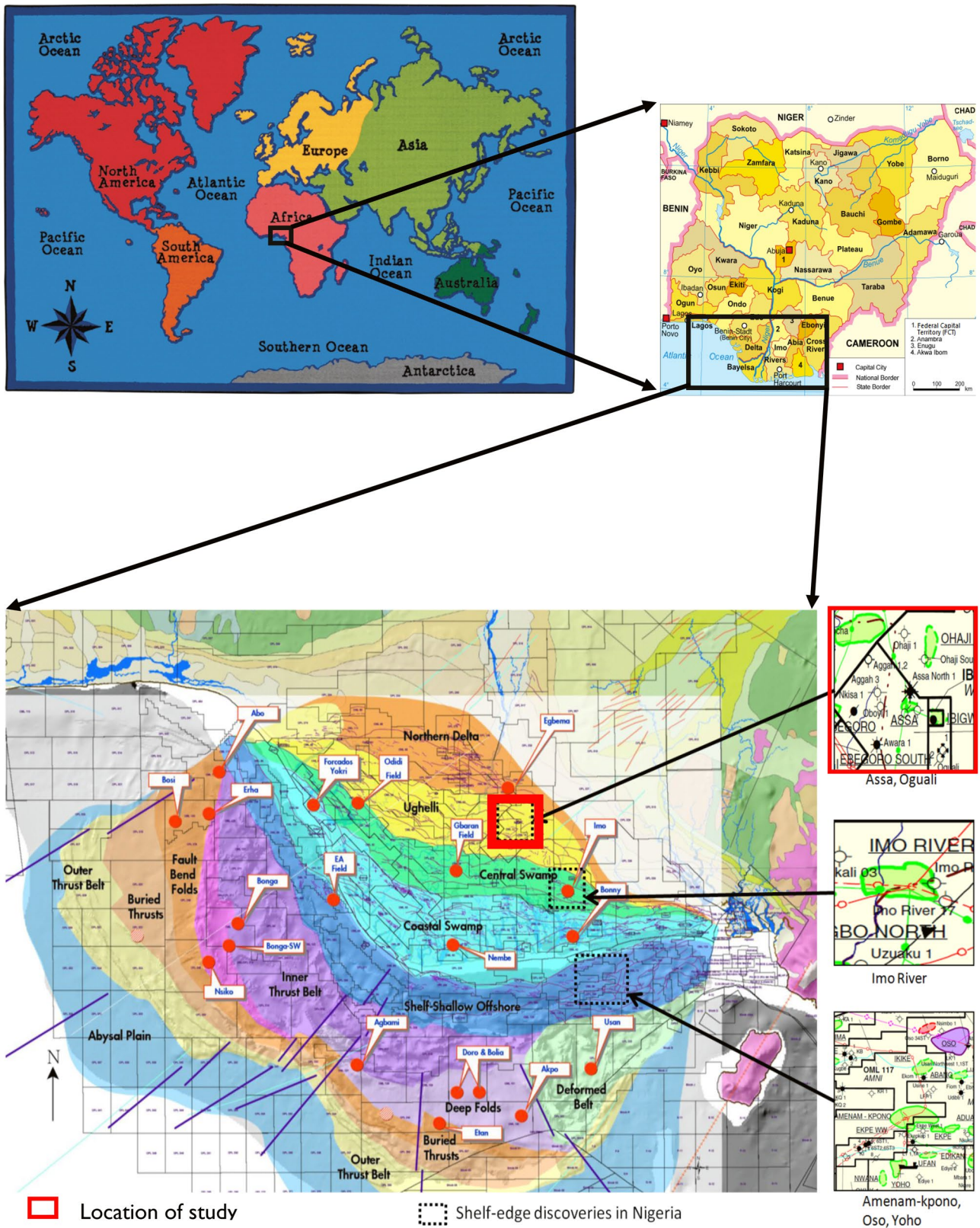2 Exploration and Development, Moni Pulo Petroleum Development Limited, Port Harcourt, Nigeria

**Fig. 1** Location of study area and compiled locations of shelf-edge delta discoveries in structural play segments map of Niger Delta Basin, Nigeria. Modified after Ejedawe et al. (2007)

associated with high accumulation of sand deposits. As a consequence, new concepts and ideas have continuously been developed in the Gulf of Mexico and other basins of the world in order to reduce the uncertainties related to the exploration and development of the resources within the shelf-edge environment.

The classification of faults with respect to their initiation, propagation, interaction and termination has been lacking in most published works in Niger Delta. Part of the problem is that there is lack of very good seismic data that will image accurately the subsurface dynamics of faults over geologic time. The proper understanding of fault dynamics has a strong implication on the geometry of sediments and their consequent abilities to provide accommodation space to massive sand deposits. Growth faults have remained the subject of extensive research since the works of Ocamb (1961), with the aim of defining their tectono-stratigraphic evolution in the context of a local petroleum system analysis. Fossen and Rotevatn (2016) attributed major growth fault evolution to initially minor ramps growing and connecting to become a major growth fault without considering the growth patterns of sediments adjacent to each fault with respect to age.

Extensional domains such as the area of focus of this study are usually characterized by listric normal faults as well as minor antithetic normal faults. Khalil and McClay (2001) proposed that extensional fault-propagation folding results in hanging-wall synclines with deposition of facies with same thicknesses across the depositional system. In the Para-Maranhao Basin, few large normal synthetic faults are associated with spectacular rollovers at the shelf-edge (Oliveira et al. 2012), while the Gulf of Mexico which has the highest shelf-edge hydrocarbon discovery is characterized dominantly by extensional growth faults. The proper understanding of fault dynamics has a strong implication on the geometry of sedimentary sequence and their consequent abilities to provide accommodation space to massive sand deposits. There is a switch from positive to negative total subsidence depending on the evolution and dynamics of the fault which over the years get deformed to form rollover structures. Sediment–load subsidence, when acting together with growth faulting, expands delta thickness significantly and results in the predominant strike alignment of shelf-edge depocentres irrespective of the delta-front regime (Xue and Galloway 1995). Doglioni et al. (1998) compared normal faulting versus regional subsidence and concluded that uniform lithology and facies changes are observed where the subsidence is less than the sedimentary fill and a lateral changes in lithology and facies are attributed to locations of higher subsidence and lower sedimentary fill. This might not always be the case in a field-scale detailed evaluation as they did not consider that at different depositional environments, the facies distribution is always never the same and also the growth, propagation of faults and structural deformation is

much likely to influence lateral stratigraphic distribution of relatively younger sediments. Studies by Obiadi and Obiadi (2016) in the Greater Ughelli Depobelt of Niger Delta shows that generally stratigraphic thickness increases in the basin-inward direction and at different stages in structural evolution, "local depocentre" has migrated from the north-west at deeper interval to south-east at shallower interval.

However, this study aims to improve the understanding of fault evolution and its implication on seismic reflection geometries, formation of depocentres and facies distribution within the Niger Delta Basin. The focus is primarily on comparing the dynamic evolution of co-planar faults and their association with sand transportation and deposition on the shelf-edge and beyond. However, other splay faults were looked at for the purpose of understanding faults evolutionary concepts.

There are a number of issues and questions regarding the shelf-edge deltas that are yet to be solved and incompletely established:

(a) Why have not the Eocene to Oligocene shelf-edge deltas of Niger Delta Basin been reported in the literature? The published reports of discoveries of shelf-edge deltas are from Miocene age.

(b) To what extent does the evolution of co-planar faults affect the stratigraphic geometry and lateral facies variations within the deltas? The studies by Adereti et al. (2012) and Fieldman et al. (2013) were based primarily on cores and well logs to delineate depositional environment and the action of wave- and tide-dominated shelf-edge deltas which result to highstand system tracts and lowstand system tracts, respectively. Their studies did not consider fault evolution.

(c) What inference does seismic reflection geometries (e.g. wedge, sigmoid) have on sediment bypass and the potential of transporting sands to the slope and the basin floor in the presence of co-planar faults of different ages?

This study provides a detailed description of Eocene to Oligocene shelf-edge deltas and consequent association with co-planar faults of relatively different ages. It analyses the sedimentation processes and the effects of different co-planar faults to sand transportation into the slope and basin floor environment. It also provides subsurface models for better understanding of shelf-edge systems.

## Geologic and structural setting

The structural evolution of the Niger Delta is dominated by step-wise progradation during a major regressive phase that continues to the recent. The Niger Delta is subdivided

into structural zones characterized by an extensional regime onshore and a contractional regime basinwards. Growth faulting dominates the structural style of the Niger Delta extensional regime, and it is interpreted to be triggered by the movement of deep-seated, over-pressured, ductile marine shale and aided by slope instability (Doust and Omatsola 1989). The successive phases of the delta growth form transient depobelts that are bounded by mega-structural growth faults. The study area straddles Greater Ughelli and Northern Delta depobelts. Much of it is in the Greater Ughelli depobelt.

Three macrostructures have been identified over the study area in the Greater Ughelli depobelt. Each macrostructure is characterized by a sandy sequence in the north which becomes shalier to the south. The classic Niger Delta stratigraphic sequence of holomarine shales (Akata Formation), fluviodeltaic sand-shale intercalation (Agbada Formation) and upper coastal plain sands (Benin Formation) is recognized throughout Greater Ughelli depobelt. Some of the regional "down-to-basin" DTB faults within the study area extended from the Older Akata Formation to Younger Benin Formation.

## Concepts and description of shelf-edge deltas

There is a range of delta types that develop across different segments of the shelf during a cycle of fall and rise of relative sea level (Porebski and Steel 2001), particularly when the fall exposes the former shelf surface. The shelf-edge or shelf-margin delta is an end member of that spectrum that becomes prominent during the falling stage of relative sea level on the shelf, but may also result from an unusually high supply of sediment at other stages in the cycle (Porebski and Steel 2003). Thus, shelf-edge deltas are a class of deltas that were developed at or near the shelf-edge environment. Shelf-edge deltas have received much attention in recent years because of major discoveries associated with them and their role as the encatchment for delivery of sediment to deep-water environments. They are well known in their geometry and morphology, especially from the Gulf of Mexico shelf-margin (e.g. Edwards 1981; Suter and Berryhill 1985; Morton and Suter 1996) and recent shelf-edge discovery in offshore Nigeria (e.g. Adereti et al. 2012; Fieldman et al. 2013). These cases show clearly that shelf-edge deltas tend to be thicker and show much more evidence of instability and collapse compared to inner-shelf deltas. The exposures from outer shelf to upper slope make it possible to analyse the variability of shelf-edge deltas in response to supply variability and to the gradient increase from outer-shelf to shelf-edge environment (Dixon et al. 2012). Research by Dixon et al. (2012) showed that river-dominated shelf-edge

deltas transport large volumes of sand to the upper slope, even when major shelf-edge incisions are absent.

The opportunity to study a complete shelf-edge system prompted investigations in Niger Delta, including seismic studies by research groups at ExxonMobil after major discoveries were made. Adereti et al. (2012) reported results of ExxonMobil investigation and provided a description of the stratigraphic composition of a classic Eastern Niger Delta discovery which found a thick stacked 1300 ft of shelf-edge reservoirs below a thick muddy high amplitude section. Anomneze et al. (2015) reported results of proven petroleum plays within the Niger Delta and interpreted shelf-edge play as a high impact prospective target for deeper exploration. The seismic reflection amplitude of the wedge encapsulating the shelf-edge deltas in Anomneze (2014) is different from that reported by the Exxon research team in shallow offshore Niger Delta. The seismic reflection amplitude of shelf-edge deltas in shallow offshore is transparent, while that of the onshore deep locations have higher amplitude. In each case, there is always a major switch in the amplitudes with a very thick muddy sequence above the deltas.

Interest in shelf-edge deltas has grown with the increased attention paid to the stratigraphic responses of depositional systems to falling relative sea level (Posamentier et al. 1992; Mellere and Steel 1995; Porebski and Steel 2003; Paumard et al. 2018). A shelf-edge delta requires its fluvial distributary channels to empty near the shelf break. This involves shoreline regression across the entire shelf and commonly implies forced regression, that is, a regression that is forced by active fall in relative sea level, and thus is independent of sediment supply (Posamentier et al. 1992). Although unusually high sediment flux combined with low-energy coast conditions may bring deltas close to the shelf break during highstands (e.g. the Balize lobe of the present day Mississippi Delta), many shelf-edge deltas have proven to be dominantly forced-regressive and lowstand features (Posamentier et al. 1992; Sydow and Roberts 1994; Adereti et al. 2012). Collapsing of a shelf-edge delta into series of rotated and tilted blocks as demonstrated, for example, in the Ubit Field, offshore Nigeria (Clayton et al. 1998), will create a disrupted slope topography that would promote the trapping of delta-derived, resedimented sands within locations relatively high on the slope.

## Dataset and methodology

The study uses a volume of 3D seismic reflection data that straddles Rivers and Imo state, well logs, checkshots, biostratigraphic (paleobathymetric, biofacies, palynological and foraminiferal zones) data. Five critical steps were selected in order to achieve the objectives of this study. All interpretation was done using Schlumberger Petrel software,

Geobody World Petrel Plug-in for geobody extraction, CorelDraw for graphic drafting and building of conceptual models. The procedure was followed systematically to arrive finally at an integrated high-resolution description of shelf-edge deltas and their associations with co-planar growth faults in the Niger Delta. These five steps are: (1) integration of well log sequence stratigraphy and biostratigraphic results, (2) seismic sequence stratigraphy, (3) gross depositional environment interpretation and geomorphological studies, (4) evolution and dynamics of growth fault interpretation, (5) shelf-edge play description and model creation.

## Integration of well log sequence stratigraphy and biostratigraphic results

From the understanding of all sequence models documented by various authors and their applicability to seismic data evaluation from a passive margin basin such as Niger Delta, the Galloway (1989) model of genetic stratigraphic sequence appears to be the best model to be adopted in the course of this study. His model overcomes the recognition problems related to correlative conformity and has the merit that maximum flooding surfaces are relatively easy to map across all part of a basin. The genetic stratigraphic sequence uses maximum flooding surfaces as boundaries, and it is subdivided into highstand, lowstand (fall and early rise) and transgressive systems tracts.

In this study, twenty-five wells were utilized for correlation of the marker events. First, a complete sequence interpretation was carried out in Asn-1 and Awa-1 wells as they had majority of the data required to get a high-resolution sequence stratigraphic framework (Figs. 3, 4). These data include gamma ray logs, resistivity logs, density logs, spontaneous potential logs, caliper logs, sonic logs, palynological and foraminiferal zones and biofacies (paly diversity PDIVERS and abundance PPOPLN with foram diversity FDIVERS and abundance FPOPLN).

The palynological and foraminiferal zones were imported into Petrel software as discrete logs and were named as P zones and F zones, respectively. The P zones available range from P630 at the top of Awa-1 well to P520 at the base of Asn-1 well. The F zones available range from F7800 at the top to F7400 at the base. The PPOPLN, PDIVERS, FPOPLN and FDIVERS were imported into Petrel as continuous logs.

The integration of the data with the marker events/shales (Table 1) from biofacies helped to pinpoint the locations of seven maximum flooding surfaces (MFSs), while five candidate sequence boundaries (SBs) were interpreted between using log motifs and the Niger Delta Chronostratigraphic Chart (Fig. 2). The SBs were mainly picked by inference using logs, while the integration of marker shales, log motifs and locations of maximum PPOLN, PDIVERS, FPOPLN and FDIVERS helped to identify the maximum flooding

**Table 1** Marker shales and ages provided from forams interpretation in the study area

| S/N | Marker Shales | Age (million years) |
|---|---|---|
| 1 | Alabammina 2 | 20.7 |
| 2 | Bolivina 26 | 23.2 |
| 3 | Alabammina 1 | 26.2 |
| 4 | Bolivina 27 | 28.1 |
| 5 | Uvigerinella 5 | 31.3 |
| 6 | Textularia 3 | 33.0 |
| 7 | Orogho Shale | 35.9 |

surfaces. This was then correlated across the other wells combining all available logs in dip (north to south) directions using the marker shales (Fig. 4). Three systems tracts were interpreted within each sequence using gamma ray log motifs as a guide, and they included highstand system tract, lowstand system tract and transgressive system tract.

## Seismic sequence stratigraphy

After a good well to seismic tie was done, faults and horizons interpretation was carried out. To carry out faults and horizons interpretation, a quick scan was done on the seismic data to ascertain which of the horizons can be interpreted continuously across the seismic data. It was observed that there are some wedge shaped geometries within the area which will affect the continuity of sequence boundaries. Therefore, the interpretation was focused on using maximum flooding surfaces as genetic bounding surfaces as it was more continuous across the seismic. The usage of maximum flooding surfaces for seismic interpretation was further validated by Embry (2009) where in his regional seismic studies in the Gulf of Mexico, he noted that most readily regionally recognizable sequence stratigraphic surface is the maximum flooding surface. In this study, maximum flooding surfaces was used appropriately to separate one sequence unit from the other in combination with biostrat data. This enabled the building of an approximate time stratigraphic framework which was essential for determining seismic reflection geometry relationships.

## Gross depositional environment interpretation and geomorphological studies

Gross depositional environment (GDE) is a summary description of the regional (mapped) distribution of depositional environments for a given chronostratigraphic interval (Mitchener et al. 1992). A GDE changes laterally and vertically in the depositional cycle. GDE interpretation in this study was carried out sequentially and by integrating well
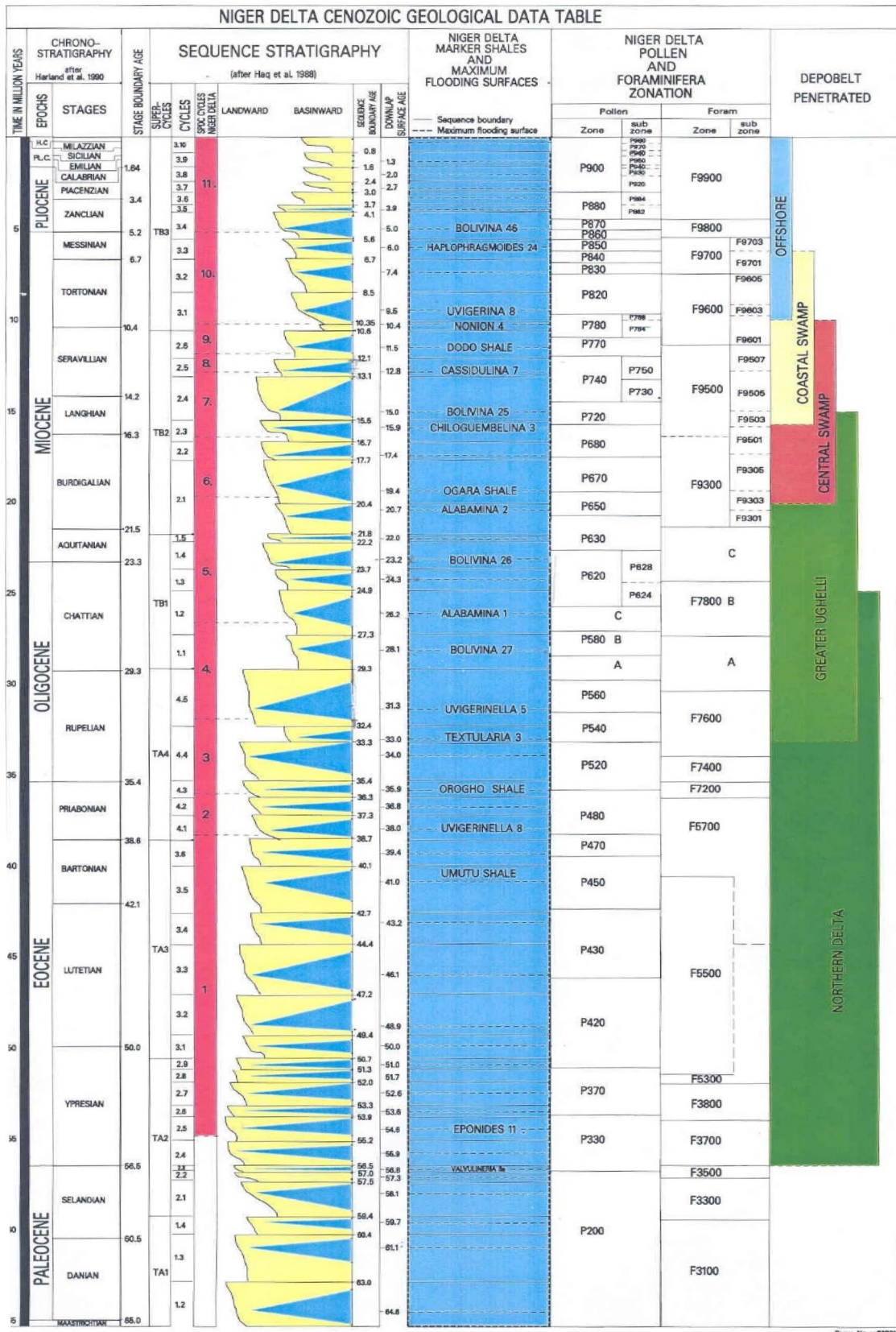
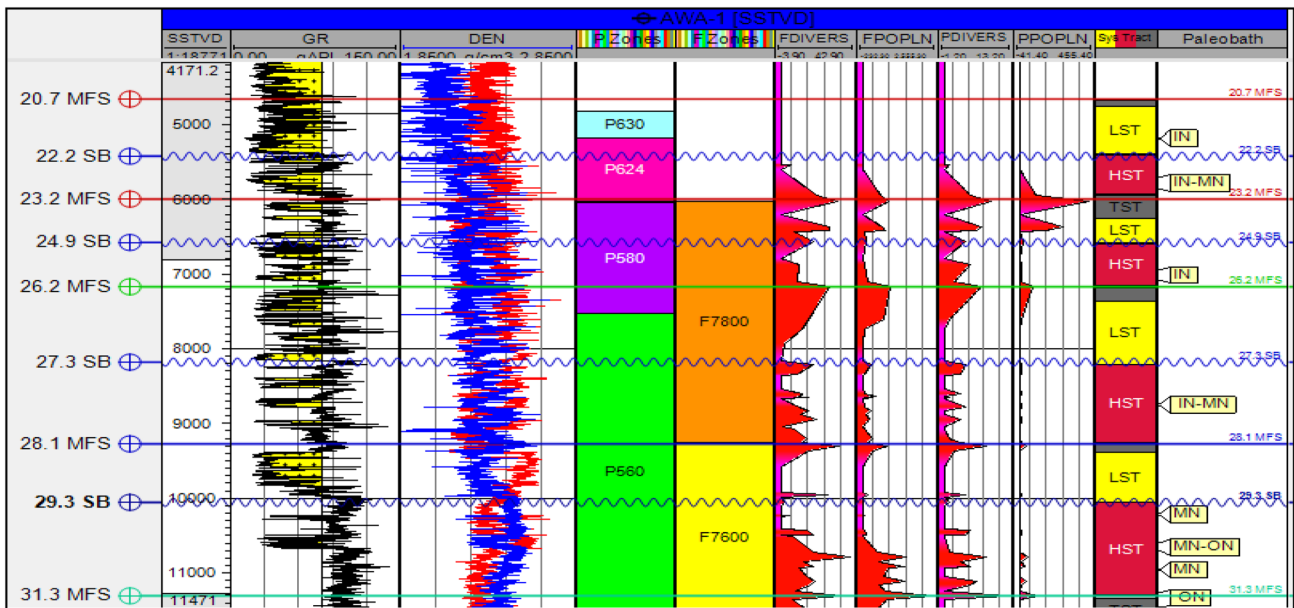**Fig. 2** Shell Niger Delta Chronostratigraphic Chart used for calibration of biostratigraphic data

**Fig. 3** Sequence stratigraphic tops interpretation using MFSs, SBs picked using gamma ray log, resistivity log, palynological and foraminiferal zones, pollen and forams diversity and population on Awa-1 well
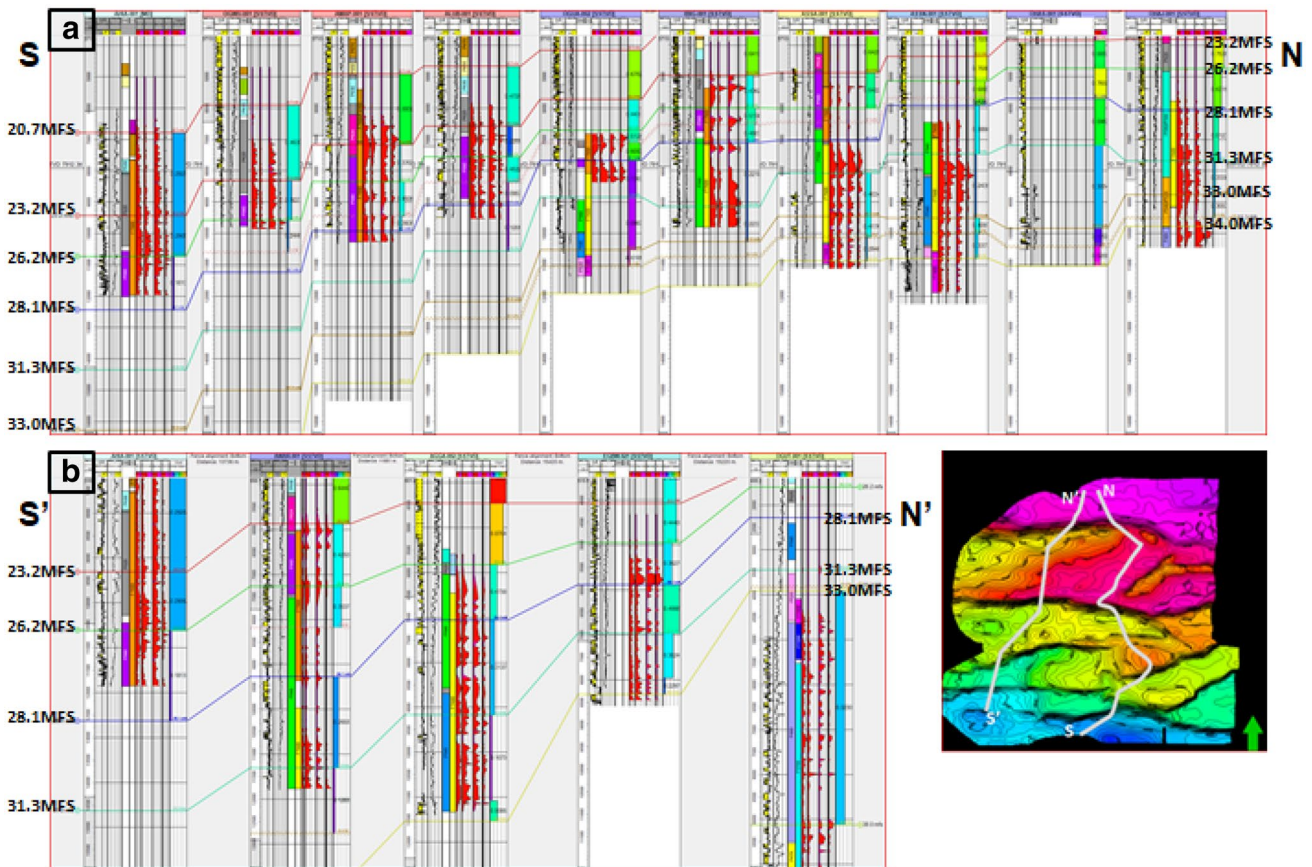


**Fig. 4** Regional sequence stratigraphic correlation along two north to south direction lines **a**, **b** with the wells used in this study

log motifs and paleobathymetric data. One of the key depositional elements that was established in each sequence is the approximate position of the shelf-slope break that defines the line separating the shelf-edge and slope GDEs. Across much of the delta where the depositional gradient is very low, it is challenging deciding where to place this break, yet its position is fundamental to the understanding of sand distribution within the shelf-edge environment. GDE interpretation in this study identified the following environment: inner-shelf, middle-shelf, shelf-edge and slope. Geomorphological studies were also carried out using geobody extractions around the shelf-edge environment and interpreting channels incisions located at the Northern/proximal portion of the study area in order to understand the reservoir feeder systems, dispersal pattern and depositional process.

### Evolution and dynamics of growth fault interpretation

The high concentration of wells and major growth faults on seismic data made this seismic volume an ideal survey for examining the interplay between fault-related sedimentation and shelf-edge systems. In addition, the regional and lateral range of facies and stratigraphic geometry changes seen in the dataset allowed for the effects of faults on sedimentation to be accounted for. The interval of interest for the analysis was from 500 ms to 3500 ms for the semblance attribute extraction. The large volume of clastic sediment deposited from Eocene to Recent has maintained an ensemble of active growth faults within the survey area.

Evaluation of the evolution and dynamics of growth fault process involved:

- Creation of semblance time slices from the shallower Benin Formation to the deeper Akata Formation. (The semblance attribute is a 3D seismic volume attribute which measures the linear coherence of events in a multi-trace seismic window, and it is specially useful for identifying discontinuities such as faults.) Followed by the adjustment of interactive opacity control on the dip direction of the newly created seismic semblance volume to better image the faults.
- Assessment of the fault traces from the semblance to correspond to actual fault on seismic lines.
- Identification of faults that exist from the shallower part of the Benin Formation to the deeper part of the Akata Formation (faults annotated in red).
- Identification of critical faults that exist from the deeper part of the Benin Formation to the deeper part of the Akata Formation (faults annotated in green).
- Identification of faults that exist from the shallow part of the Agbada Formation to the shallow part of the Akata Formation (faults annotated in blue).

- Computation of growth fault indexes to compare thickness of sediments on the hanging wall to that on the footwall in order to have an understanding of the dominant growth age associated with each co-planar fault. Studies by Gibbs (1983) show that the variation in growth index values can define the growth age and period from which a fault activity started. Growth fault index is defined as the ratio of the hanging-wall sequence thickness to the footwall thickness of the same sequence adjacent to a growth fault. The largest growth index value indicates the time a fault activity started.
- Taking seismic traverse sections along each category of fault and creating a conceptual formation pattern.
- Analysis and conceptualization of early, mid- and late stages of evolution of different faults.

It is expected that the point of origination of a fault or fracture failure initiation point will be the point of most active growth in the fault system and this is reflected in the vertical growth of sediments across the fault as the thickest sediment will be associated with this initiation point. Also, as faults propagate and grow over time, they tend to influence/initiate faulting activities around them and dominantly in the direction of their propagation. All these concepts were used to create subsurface structural models that will realistically predict fault interactions and its relation to sedimentation.

### Shelf-edge play description and model creation

Detailed criteria for Niger Delta Eocene to Oligocene shelf-edge play identification and understanding were developed from this study using the gross depositional environment analysis, identified co-planar faults dynamics and their associated lithofacies variability. Complete description of shelf-edge play and their stratigraphic distribution with regard to faulting was evaluated and used to create conceptual models comparing two co-planar faults evolution and their impact in providing accommodation space to sediment deposition and the possibility of transporting sands down to the basin.

### Results and discussion

Twenty-five wells were used for correlation of the marker events. First, a complete sequence interpretation was carried out in Awa-1 well as it had majority of the data required to get a high-resolution sequence stratigraphic framework (Fig. 3). For the shallower sequences, the marker events were picked with other distal wells (having higher shale intercalations and biostrat data) which depicted where the corresponding MFSs and SBs should be.

The integration of the well logs with the marker events/ shales (Table 1) and biostratigraphic data helped to pinpoint the locations of seven maximum flooding surfaces, while five sequence boundaries (base of thick sand) were interpreted between using log motifs and the Niger Delta Chronostratigraphic Chart as a guide.

This was then correlated across the other wells combining all the logs in dip (north to south) directions using the marker shales (Fig. 4). Six sequences were established from MFS 20.7 to 35.9. It was observed that generally, as sediments move from north to south, the sequences become sandy in the north and shaly towards the south. Three system tracts have been interpreted within each sequence using gamma ray log motifs, and they include highstand system tracts HST, lowstand system tracts LST and transgressive system tracts TST. In each sequence, the HST is separated from the LST by a sequence boundary, while the TST is separated from the HST by an MFS. The LST is marked by sea-level fall which results into blocky and fining upwards sands, and HST marks a combined aggradation and progradation processes, while the TST marks a complete transgressive phase of deposition dominantly made of shale.

In this study, seven maximum flooding surfaces have been interpreted on seismic (MFSs 23.2, 26.2, 28.1, 31.3, 33.0, 34.0 and 35.9) in order to help image the lateral facies

changes and to identify facies that correspond to reservoir prospective areas (Fig. 5). The seismic facies analysis approach uses seismic reflection geometries and amplitudes as seen on vertical transects to define seismic facies that are linked to specific stratigraphic bodies which can be used to make qualitative lithology predictions away from existing well control. Seismic facies identification in this research was carried out adopting the Prather et al. (1998)-type convention and uniquely classifying them from our seismic reflection, log motifs and sand percentage interpretation. Seismic facies interpretation was carried out based on three primary parameters (reflection amplitude, reflection continuity, reflection patterns) along key seismic traverse to identify the seismic facies indicative of exploration play facies (Fig. 6). Some significant seismic reflection geometries were identified on the traverses which includes wedges, sigmoid and downlaps. In this study, downlaps have been identified as events that terminate on the maximum flooding surfaces, while some of the wedges here are suggestive of the presence of earlier fault formation process. Much of the sands have been identified to be located towards the base and tops of the wedges which provide a predictive framework for exploration of reservoirs within such wedges. Four seismic facies have been identified from the traverse section, Cbh (high amplitude convergent), Cbl (low amplitude convergent), Bl
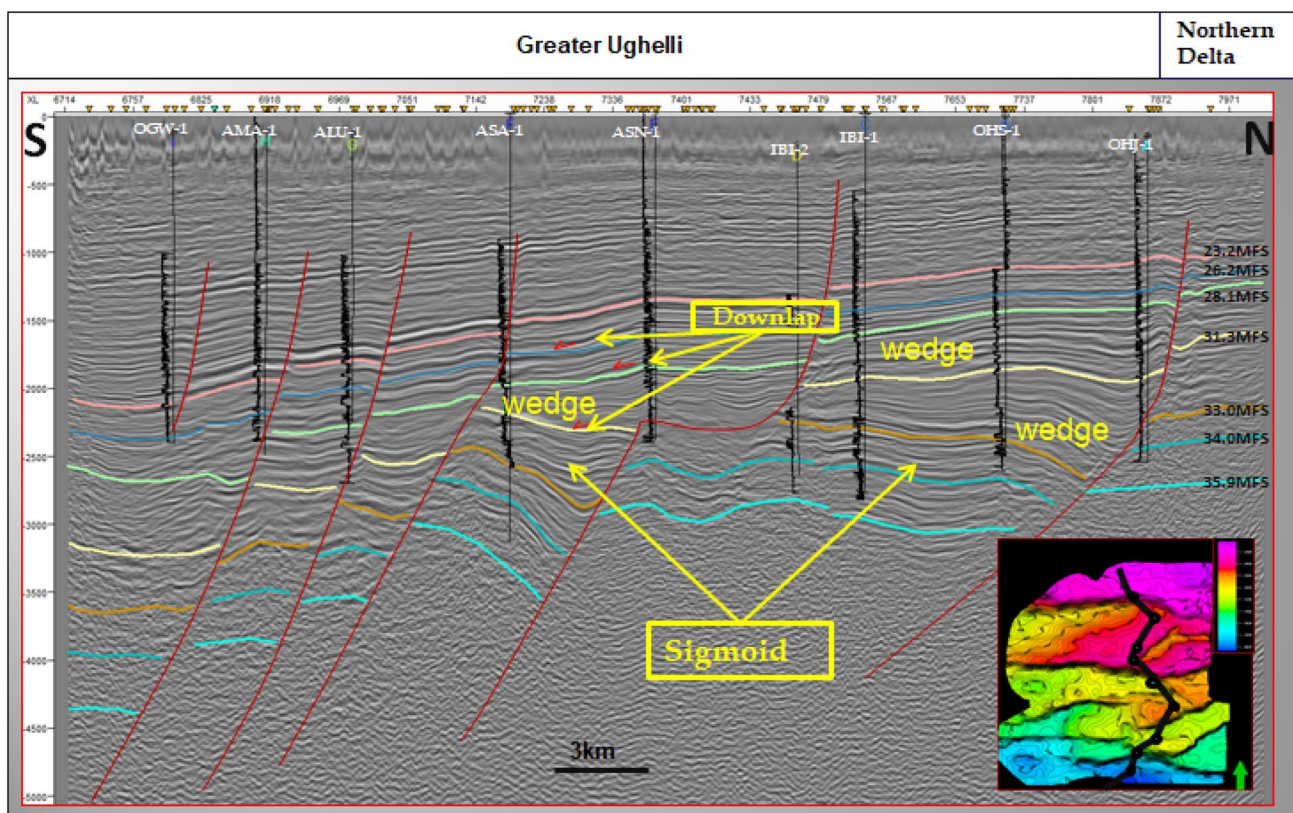


Fig. 5 Seismic stratigraphic section of the study area with stratal geometries indicating the presence of wedges
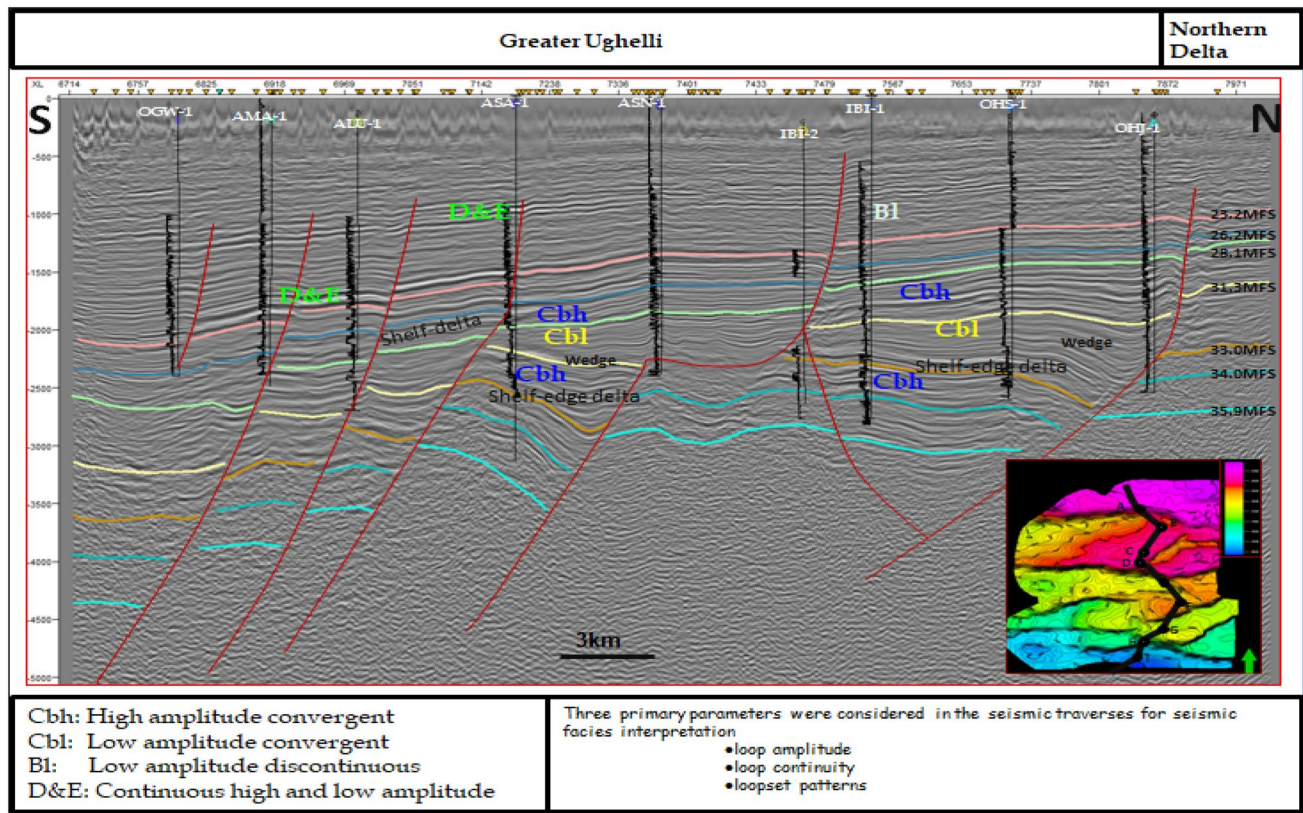
**Fig. 6** Seismic stratigraphic section of the study area with seismic facies indicating the presence of Cbh, Cbl, Bl and D&E facies

(low amplitude discontinuous), D&E (continuous high and low amplitude).

Gross depositional environment interpretation was carried out using lithofacies logs and paleobathymetric data from each sequence. The sequences of focus were those that had more well data and also those that were primarily from the Agbada Formation (which comprises of major sand and shale intercalations), and they include sequences 26.2 MFS to 28.1 MFS, 28.1 MFS to 31.3 MFS, 31.3 MFS to 33.0 MFS, 33.0 MFS to 34.0 MFS. The interest of carrying out the gross depositional environment is to be able to identify and confirm the areas that correspond to shelf-edge environment. It was suggested by Steel et al. (2000) that the key to recognizing older shelf-edge deltas is in the correct identification of the ancient shelf-edge environment. This was carried out using depositional environment chart in Fig. 7 as a guide. There is a systematic change of lithofacies and paleobathymetry as we move from one gross depositional environment to another. The lithofacies are obtained from gamma ray logs which shows that the left deflection of gamma ray logs indicate sands, while deflection to the right indicates the presence of shale. The paleobathymetric reports from each sequence were utilized, and they were mainly of the following burial ranges: inner neritic IN, inner neritic to middle neritic IN-MN, middle neritic, middle neritic to outer neritic MN-ON, outer neritic ON and bathyal BA. The integrated interpretation of the lithofacies and paleobathymetry (Fig. 8) shows that there is a significant lithofacies and paleobathymetry change as sediments move from north to south which resulted in five gross depositional environments: inner-shelf, inner- to middle-shelf, middle-shelf, shelf-edge and slope (Fig. 9).

The inner-shelf environment is dominantly of cleaner sands within a paleobathymetry of inner neritic. The inner to middle-shelf environment comprises of minor shales and major sands within a combined paleobathymetry of inner neritic to middle neritic. The middle-shelf environment comprises of shales and major sand intercalations within a paleobathymetry of middle neritic. The shelf-edge comprises of isolated sand deposits that have numerous shale intercalations within a paleobathymetry of middle neritic to outer neritic. The slope environment in this study was inferred using the understanding that after the shelf-edge, the next environment to expect is the slope with a dominant paleobathymetry of bathyal having minor stacks of sands with massive shale deposits.

The shelf-edge environment has been identified to occur within three sequences 28.1 MFS to 31.3 MFS, 31.3 MFS to 33.0 MFS and 33.0 MFS to 34.0 MFS as shown in Fig. 9 (coloured in green). The results from the gross depositional
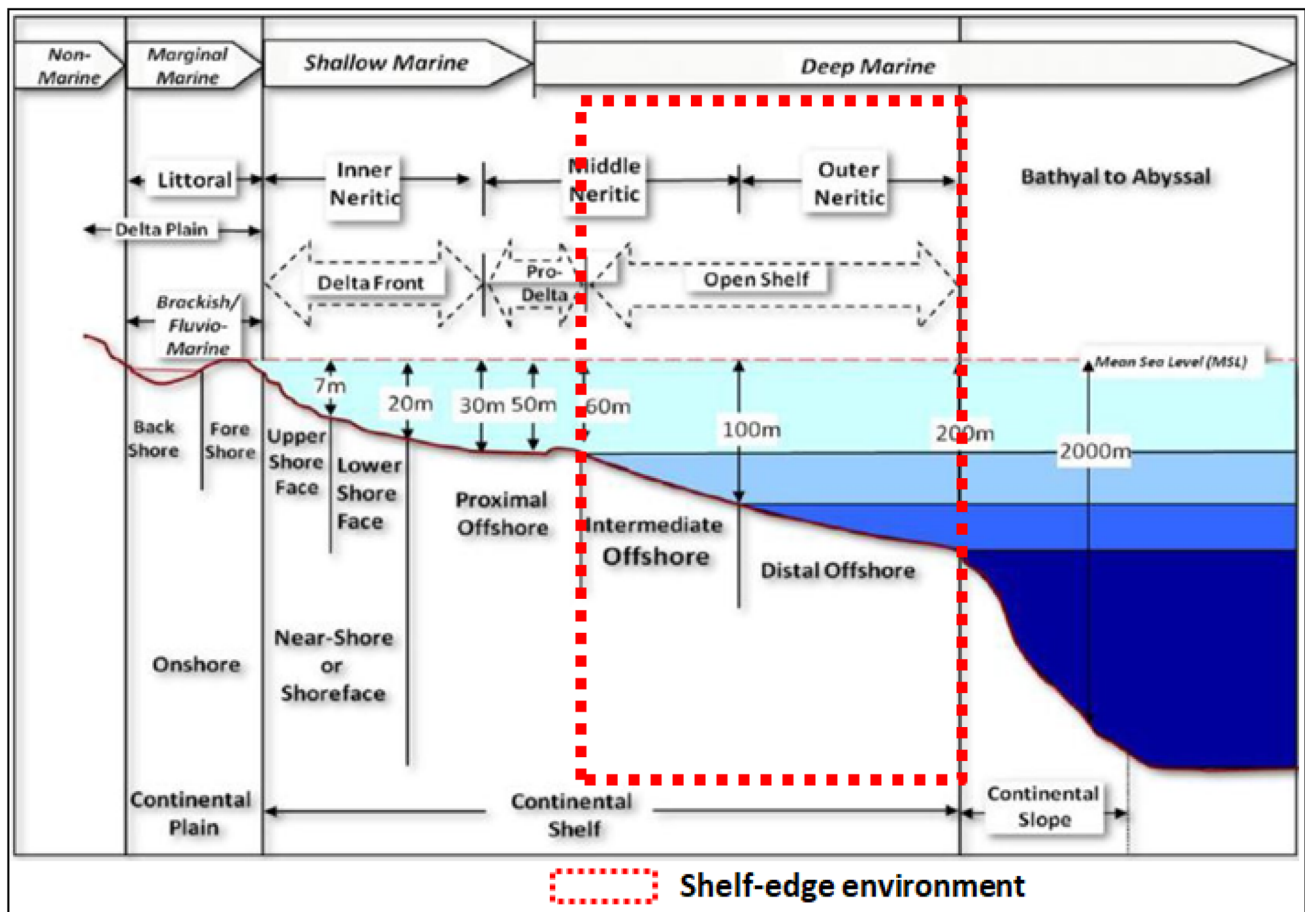
**Fig. 7** Location of shelf-edge environment. Modified from Allen (1965)

environment maps will help to streamline the interest areas in building shelf-edge models and their relationship with growth faults.

Geomorphological studies were carried out within the study area and up-north away from the study area. The reason for carrying out geomorphological studies towards the northern portion of the fields is to be able to see the possibility of mapping channel incisions that could serve as the feeder systems for the area of study as the works of Porebski and Steel (2003) and Paumard et al. (2018) have shown that for sands to be transported to the shelf-edge and farther into the basin, there is need for the presence of channel incisions towards the proximal axis of the prospective zones and if more channels can be identified at the shelf-edge, it increases the amount of confidence in sand transport towards the slope and down to the basin. However, in the Eocene examples of Steel et al. (2000) and Plink-Bjorklund et al. (2001), shelf-edge deltas are common features of the shelf-margin, especially during time intervals when the shelf-edge area was not canyonised.

A geobody interpretation was carried out within the sequences of interest that infers shelf-edge environments

from MFS 28.1 to 34.0 with dominant extraction from 28.1 to 31.3 MFS. This involved the use of selected threshold values that corresponds to amplitudes of the hydrocarbon-bearing reservoirs to run a prediction algorithm away from well control. Series of geobodies was extracted, and they indicate locations of hydrocarbon-bearing sands within the study area (Fig. 10).

The two identified geobodies towards the southern portion are associated with the faults F2 and F7. The geobody associated with F2 (red in colour) looks localized, while that associated with F7 (purple) shows that the sands must have travelled farther.

The geomorphological study carried out northwards was in the Izombe Field. Seismic data from Izombe Field were used for this purpose. There are so many seismic incisions in the Izombe field, and a few has been identified and mapped out within the Izombe seismic using two transect sections (Figs. 11, 12). These provide enough confidence in chasing for reservoirs within the fields of study and secondly will add value to the final conceptual models that leads to the deposition of shelf-edge delta reservoirs and possible prediction of sand transportation and deposition down to the
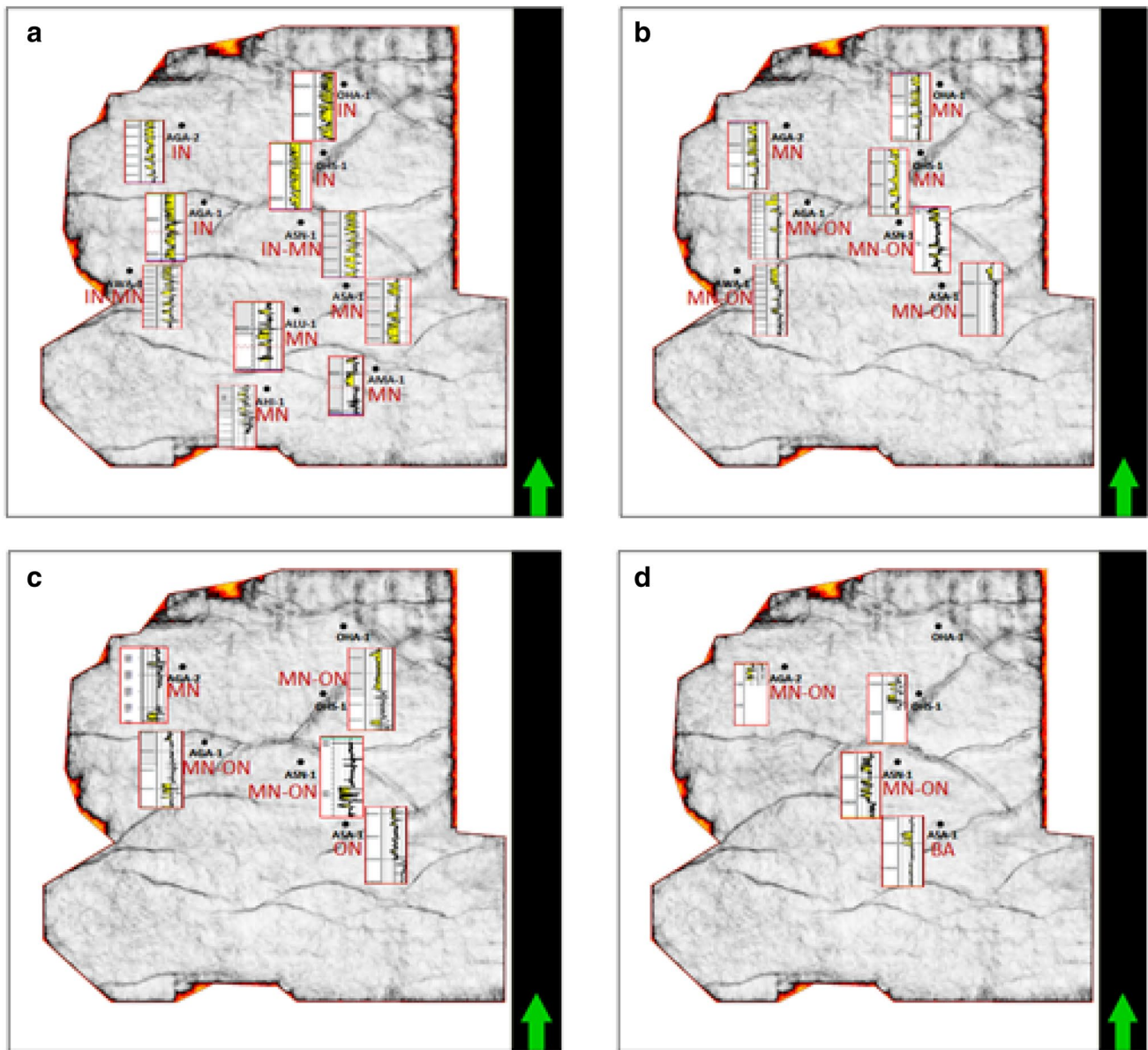
**Fig. 8** Lithofacies using gamma ray log and paleobathymetric interpretation using *IN* inner neritic, *MN* middle neritic, *ON* outer neritic, *BA* bathyal, from **a** MFS 26.2 to 28.1, **b** MFS 28.1 to 31.3, **c** MFS 31.3 to 33.0 and **d** MFS 33.0 to 34.0

basin considering Porebski and Steel (2003) and works of Paumard et al. (2018).

In order to further analyse and conceptualize early, mid- and late stage evolution of the different faults inherent in the seismic, the fault regions were classified into two segments of interest—segment A and B (Fig. 13).

The segment A is the primary focus of this study of which we are considering two co-planar adjacent faults (F2 and F7) in order to identify which of the two faults were precursor to the other. This requires careful analyses of the semblance slices, growth fault indexes and traverse sections. From the semblance slices, it is observed that the F2 is a regional fault

that cuts through from Akata Formation and terminates at the shallow part of the Benin Formation, while F7 is only found to exist from Akata to Agbada Formation. Figure 14 shows semblance slices and fault image variation from 500 to 4000 ms indicating that the F2 red fault becomes visible at semblance slice of 500 ms, while F7 only becomes visible at a more deeper semblance slice.

The concepts of Oliveira et al. (2012) were adopted in identifying the major seismic reflection growth position from three stratigraphic units along seismic traverses. The major growth strata have been identified as a key criteria for distinguishing the ages of different growth faults, as the
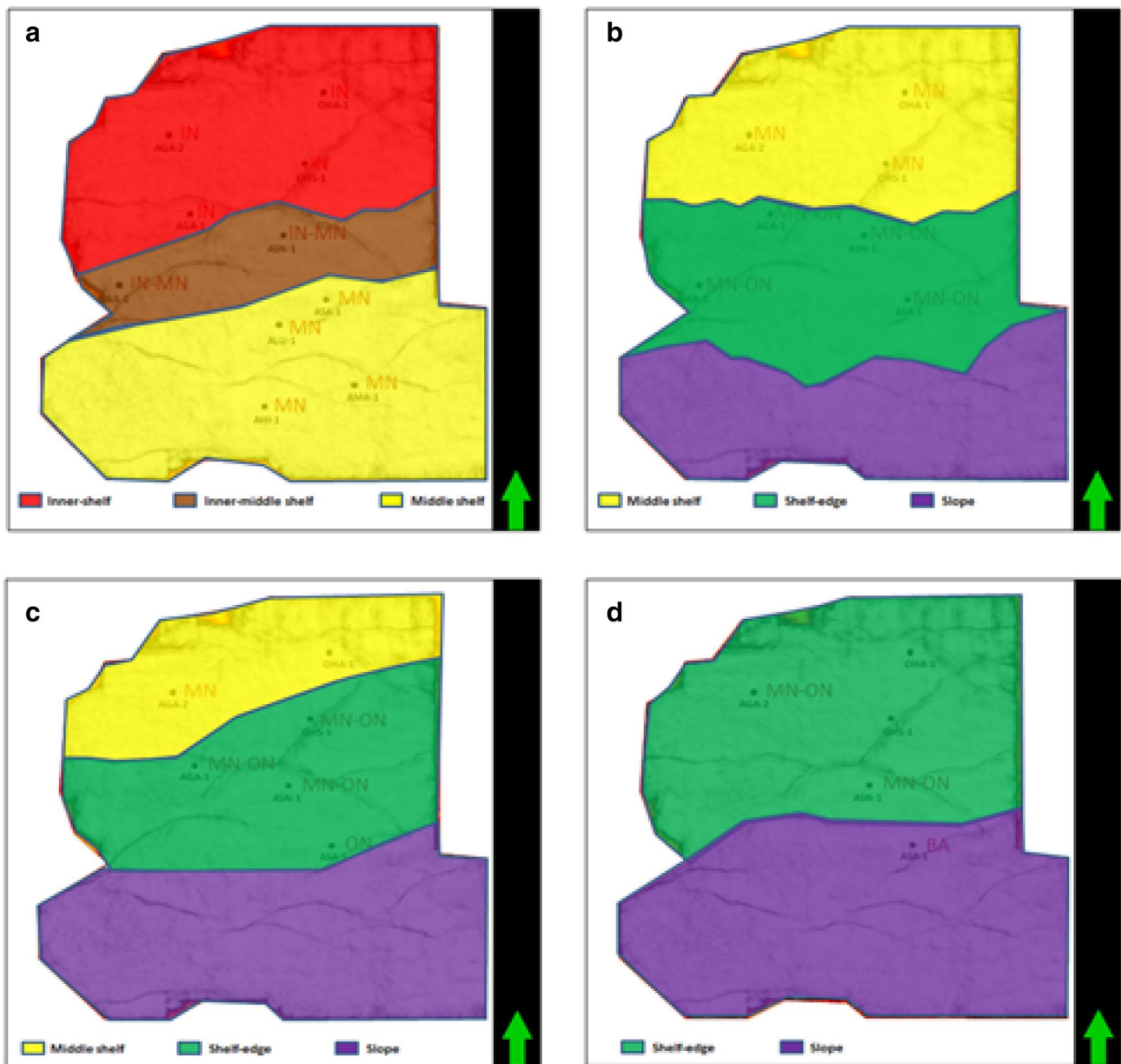
**Fig. 9** Resultant gross depositional environment maps from **a** MFS 26.2 to 28.1, **b** MFS 28.1 to 31.3, **c** MFS 31.3 to 33.0 and **d** MFS 33.0 to 34.0

major growth sequences are associated with the relatively older fault and consequently reflect the period when fault activity started. To evaluate the major stratigraphic growth position and understand the pre-growth and growth stages of the sequences within the study area, a combined analysis was carried out using growth fault index computation, thickness maps (isopach) creation and the interpretation of thickness variation of selected transect sections.

In order to compute the growth fault indexes of the sequences that was intercepted by fault 2 and fault 7, it was necessary to create seismic transect sections which

helped to individually calculate the thickness of sequences adjacent to fault at the footwall and the corresponding thickness of same sequences at the hanging wall (Fig. 15). Results of the growth fault indexes are shown in Tables 2 and 3.

From the growth fault index computation, it was deduced that the sequence with the largest growth index corresponds to the age at which the fault activity started. Thus, from the growth index results as shown in Tables 2 and 3, respectively, it shows that F2 started forming from 31.3 to 33.0 MFS, while F7 started forming from 28.1 to 31.3 MFS.
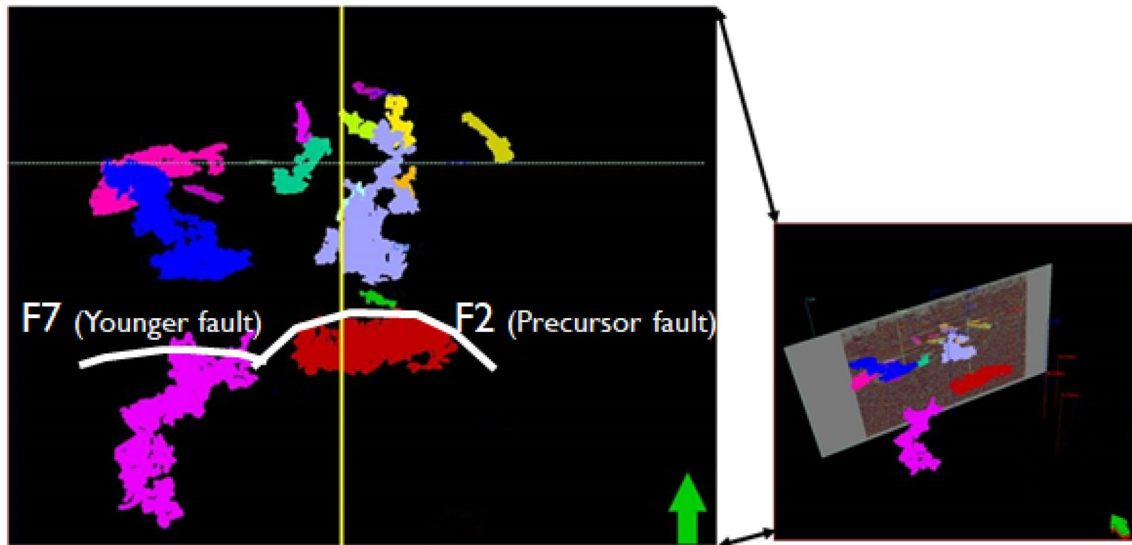
**Fig. 10** Geobodies extracted within the study area with co-planar faults overlay
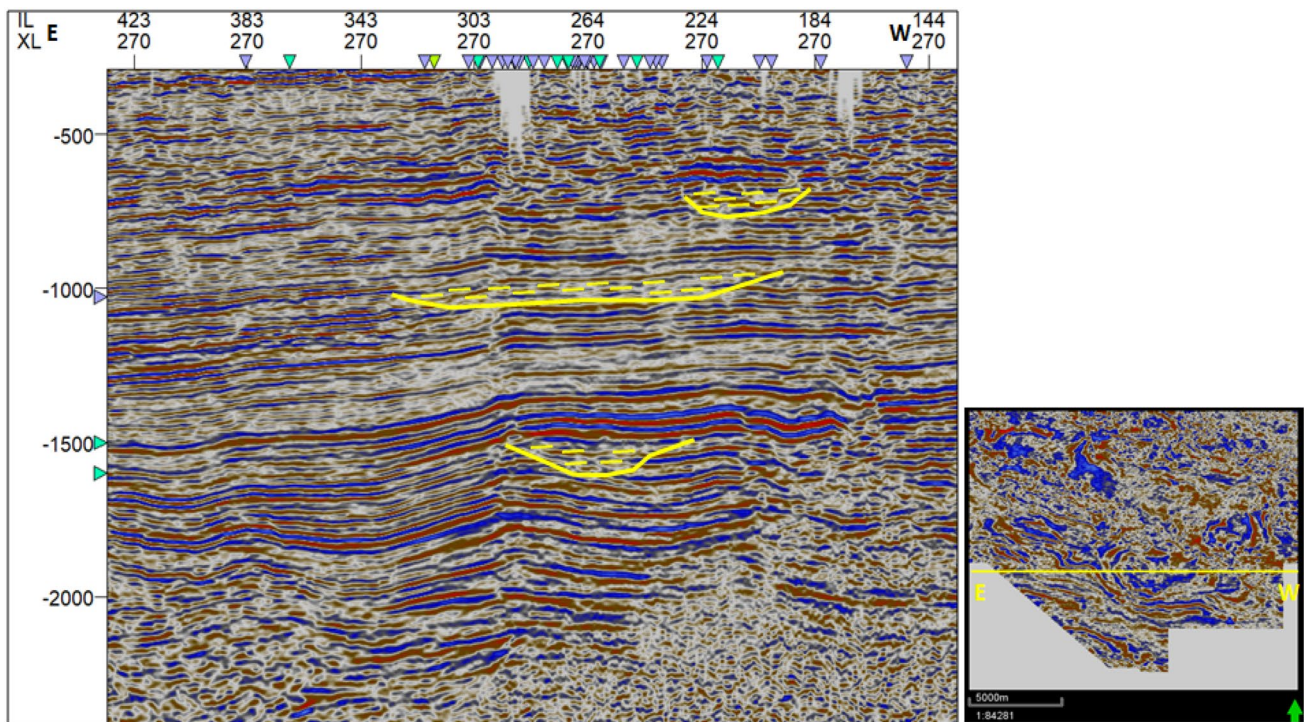


**Fig. 11** Channel incisions up-north from Izombe seismic survey—line 1

Hence, it shows clearly that relatively fault 2 is an older fault (precursor) as compared to fault 7.

This was also corroborated by the creation of thickness maps (isopachs) which showed that during the ages of MFS 33.0 to 34.0, a pre-growth period was recorded as there was no significant depocentre (Fig. 15a). However, within the

age of MFS 31.0 to 33.0, a major depocentre was formed at the hanging wall of fault 2 reflecting a major sedimentary growth (Fig. 15b), while comparatively at the hanging wall of fault 7, there was no depocentre. This confirms that fault 2 started forming before fault 7. Within the ages of MFS 28.1 to 31.3, a major depocentre was formed at the hanging wall
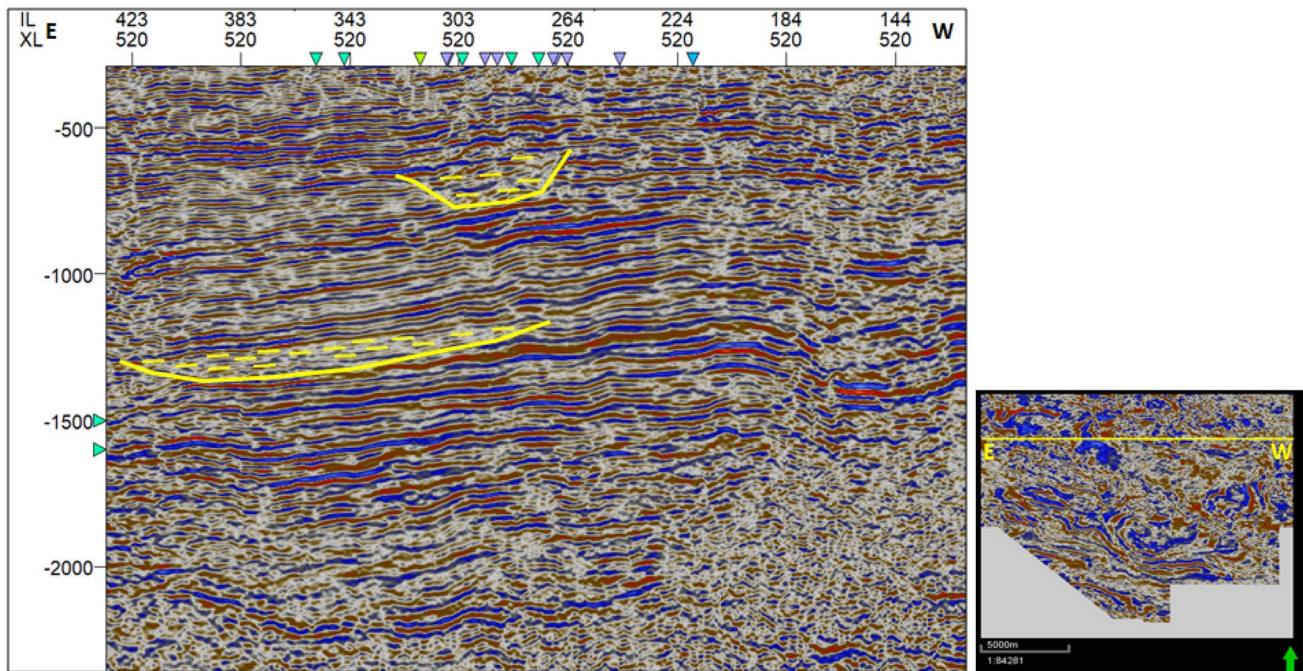
**Fig. 12** Channel incisions up-north from Izombe seismic survey—line 2
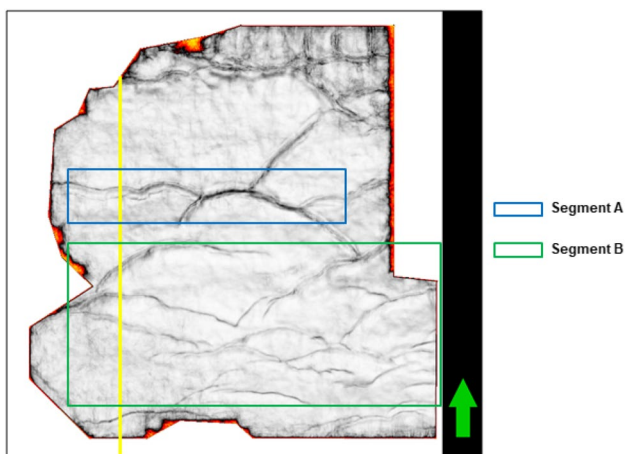


**Fig. 13** Study area segments used for fault dynamics interpretation

of fault 7 which increases further in the basinward direction, while comparatively at the hanging wall of fault 2, there was a depocentre that reduces in thickness towards the basinward direction (Fig. 15c).

From the traverse sections in Fig. 16, it was observed that F2 has its major stratigraphic hanging-wall growth thickness from 28.1.0 MFS to 33.0 MFS, while F7 has its associated major stratigraphic hanging-wall growth thickness to be from 23.2 MFS to 31.3 MFS. This also implies that F2 was a precursor fault that was formed before F7. It is also likely that F2 initiated the formation of F7. A conceptual framework was created to describe the fault formation (Fig. 17) which shows that the paleo-stress direction is towards the western part of the segment A. It also infers that the precursor faults provide more accommodation space for sand deposition than the younger co-planar fault during deposition, coarser sediments are deposited faster than finer sediments; thus, more sands are deposited at the base of the wedges/depocentres in F2.

Conceptual models were developed from the fault evolution analysis from Figs. 14, 15, 16 and 17 which shows that there are three stages in fault activity: pre-growth, growth and post-growth faulting processes (Fig. 18). The major growth strata aid the determination of relative ages of faults (Fig. 19).

## Shelf-edge play description and model creation

The integration of sequence stratigraphy, fault evolution and gross depositional environment has aided shelf-edge delta interpretation (Fig. 20). Sequence 28.1–31.3 MFS was used for this purpose since a notable position of shelf-edge environment has been interpreted within this sequence; the sequence has enough data for calibration, and the two primary faults of interest (F2 and F7) can be found to be within the shelf-edge region of this sequence. There is an increase in reservoir thickness and net to gross in the proximal part of the sequence associated with precursor (older) fault F2, while towards the distal part, reservoir thickness gradually reduces with faster thinning rate at the base. There is also a
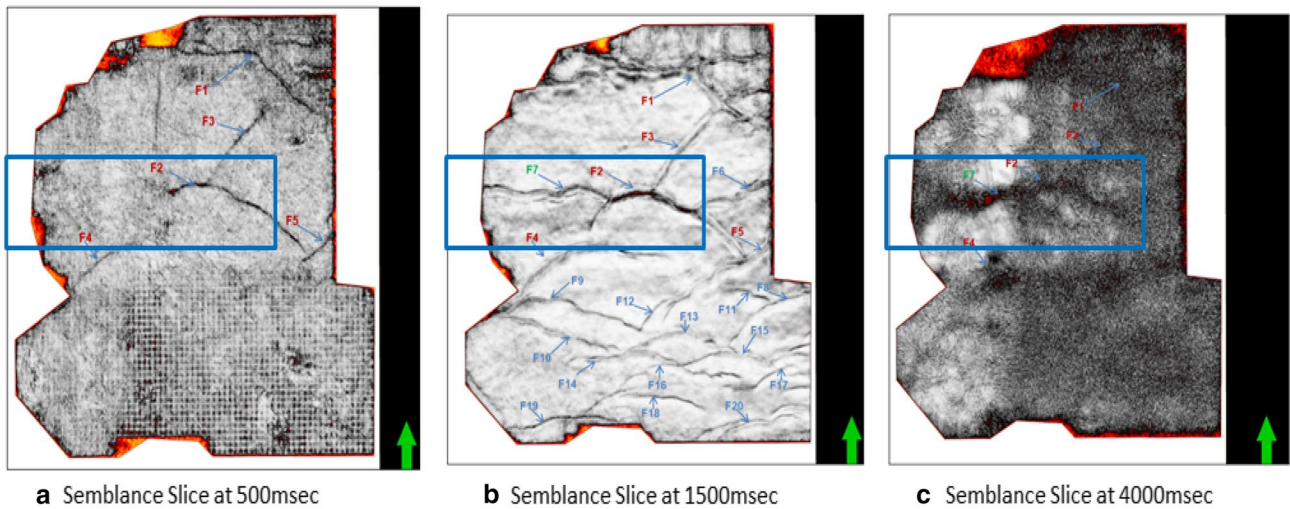
Springer

**a** Semblance Slice at 500msec  **b** Semblance Slice at 1500msec  **c** Semblance Slice at 4000msec

**Fig. 14** Semblance slices indicating variation in fault existence from 500 to 4000 ms
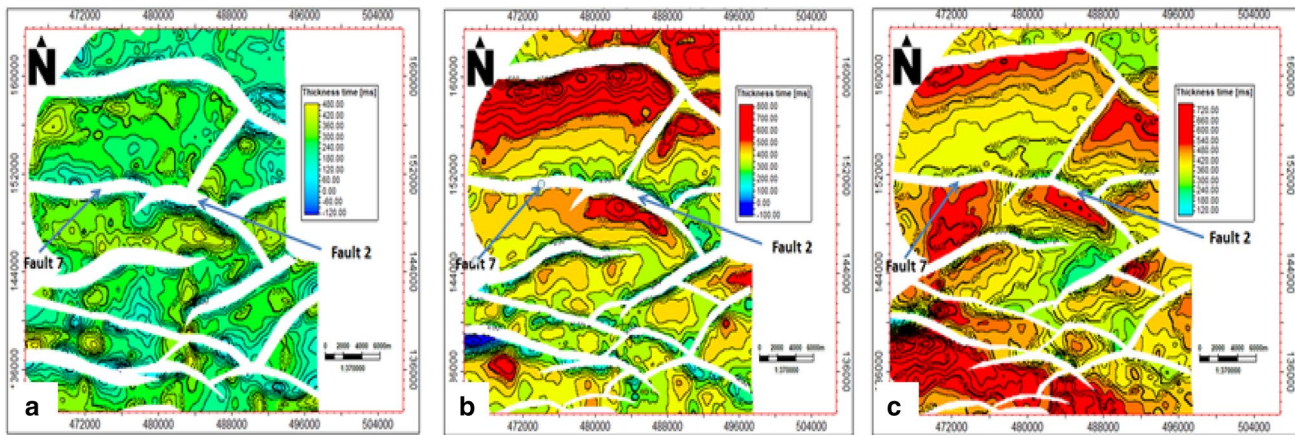


**Fig. 15** Thickness map (isopach) of **a** MFS 33.0–34.0 showing pre-growth stage, **b** MFS 31.3–33.0 showing major growth stage of fault 2 adjacent sediments, **c** MFS 28.1–31.3 showing major growth stage of fault 7 adjacent sediments and minor growth stage of fault 2 adjacent sediments

| Sequence (MFS) | Footwall thickness (FWT) | Hanging-wall thickness (HWT) | Growth index (HWT/FWT) | Remarks |
|---|---|---|---|---|
| 23.2–28.1 | 404.9 | 510.0 | 1.260 | |
| 28.1–31.3 | 350.3 | 444.5 | 1.269 | |
| 31.3–33.0 | 284.9 | 552.5 | 1.939 | Age of Fault 2 |
| 33.0–34.0 | 223.6 | 253.0 | 1.131 | |
| 34.0–35.9 | 309.9 | 345.0 | 1.113 | |

**Table 2** Growth fault index computation for fault 2 showing the age at which fault 2 started forming

relative decrease in reservoir thickness and net to gross in the proximal part of the sequence associated with younger initiated fault F7, while towards the distal part, it gradually increases in reservoir thickness and net to gross (Fig. 20). From system tracts interpretation, the thickest sands of this sequence of interest are located towards the top and are features of lowstand system tracts, while the minor sands located towards the base of this sequence are of highstand system tracts. This infers that at the shelf-edge environment, the thickest sand will be as a result of major sea-level fall which marks the lowstand system tracts. Representative conceptual models of the lithofacies, net-to-gross and

**Table 3** Growth fault index computation for fault 7 showing the age at which fault 7 started forming

| Sequence (MFS) | Footwall thickness (FWT) | Hanging-wall thickness (HWT) | Growth index (HWT/FWT) | Remarks |
|---|---|---|---|---|
| 23.2–28.1 | 365.6 | 419.4 | 1.147 | |
| 28.1–31.3 | 334.4 | 547.7 | 1.638 | Age of Fault 7 |
| 31.3–33.0 | 385.8 | 492.0 | 1.275 | |
| 33.0–34.0 | 238.2 | 256.0 | 1.075 | |
| 34.0–35.9 | 343.6 | 403.0 | 1.173 | |
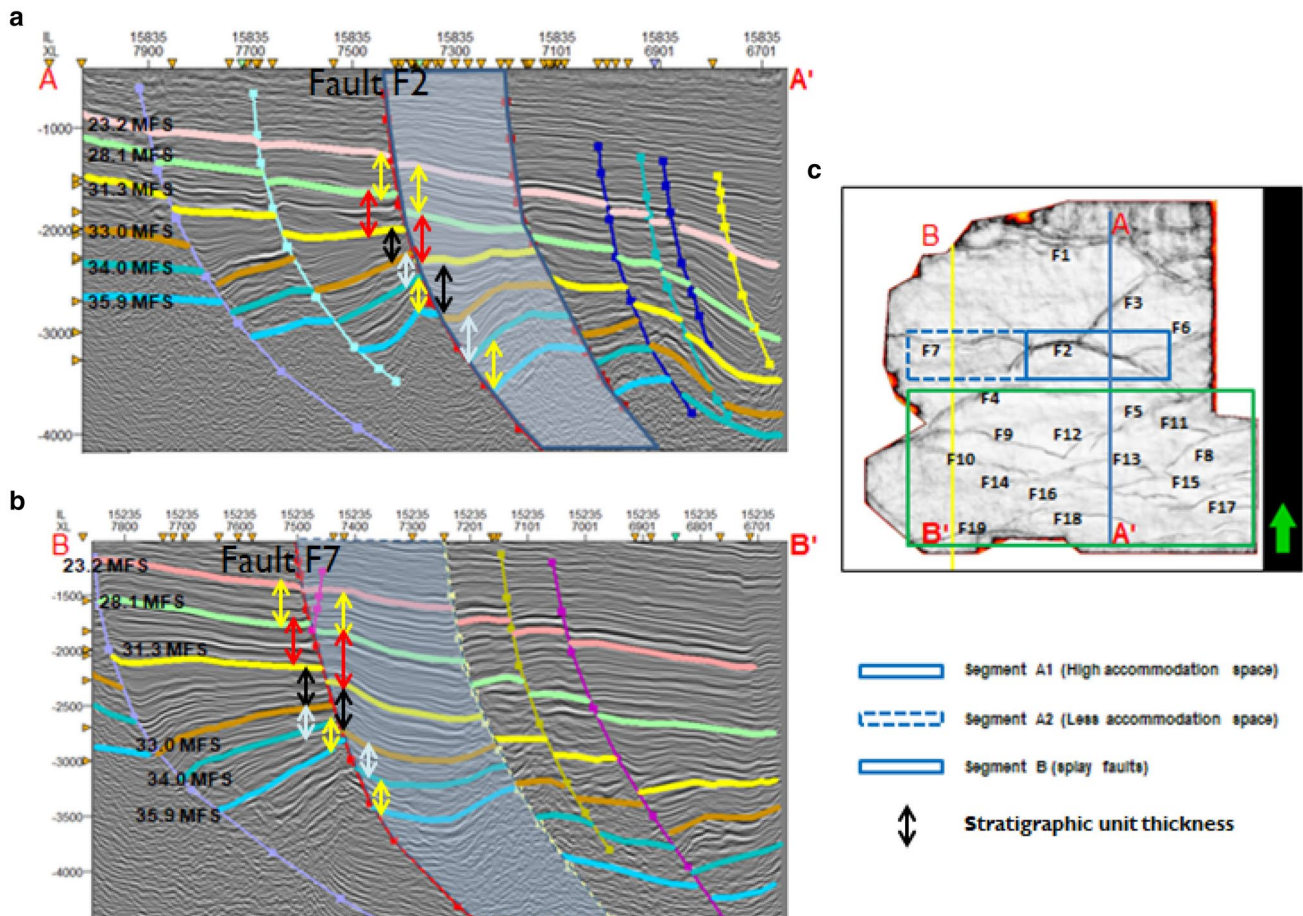


**Fig. 16** Seismic traverses showing different growth faults and respective stratigraphic geometries **a** line A–A′ showing fault 2 adjacent stratigraphic relationship in segment A, **b** line B–B′ showing fault 7 adjacent stratigraphic relationship in segment A, **c** semblance slice showing the names of the various faults and segments

accommodation (from axis of subsidence) variation have been created from this study (Figs. 21, 22). The axis of subsidence shows the points of maximum sediment deposition which will accommodate more sands.

As a delta reaches the shelf-edge and begins to prograde onto the upper slope, there is a significant change in facies development, due to the increased gradient of the substratum (Mayall et al. 1992) which is evident in Fig. 20. On the basis of his work in the Paleocene–Eocene Rosita delta system in the Gulf of Mexico, Edwards (1981) suggested that

inner-shelf deltas tend to be "horsetail" and develop a wide delta-front sheet sand, whereas those that reach the shelf break are characteristically locally thickened in the presence of growth faults. Edwards (1981) did not consider and compare that the age and evolution of growth faults could have effect on the amount of thick sands that will be found at the shelf-edge. Tectono-depositional conceptual models have been created in this study using the information from Figs. 20, 21 and 22 and the gross depositional environment maps and geobody interpretation. The first model (Fig. 23)
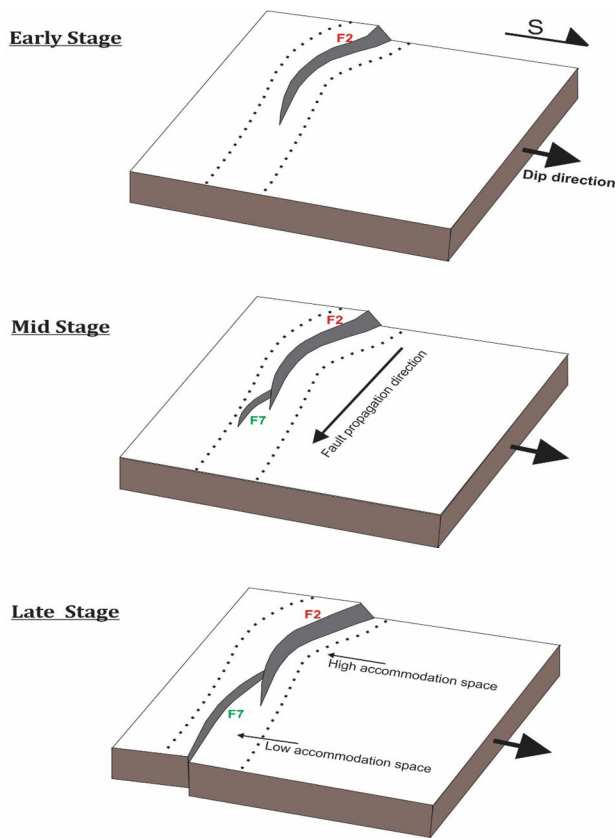
**Fig. 17** 3D view of segment A showing the evolution and propagation of fault from east to west direction (precursor faults result in higher accommodation space, while newly initiated fault results in lower accommodation space)
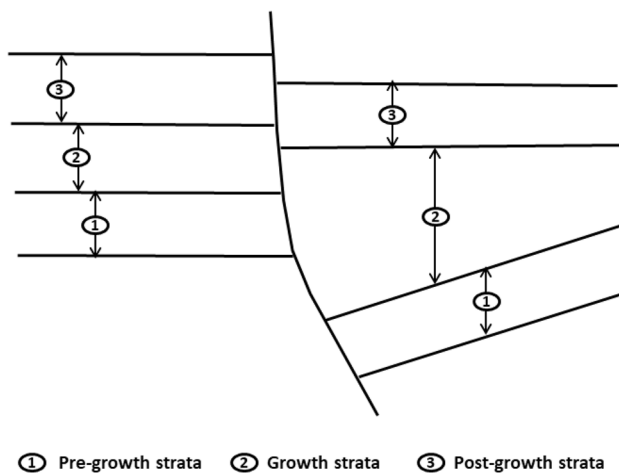


**Fig. 18** Concept of pre-growth, growth and post-growth strata

represents sand transportation and deposition from the inner-shelf to the basin in the presence of a younger fault. It shows evidence that during sediment transportation, in the absence

of a fault at the shelf-edge environment having a gentle slope (Fig. 7), sands are transported farther into the basin floor in the form of basin floor fans.

The second model (Fig. 24) represents sand transportation and deposition from the inner-shelf to the slope. It shows evidence that during sediment transportation, the presence of growth fault at the shelf-edge tends to create big accommodation space having a steep slope; thus, much sands are deposited in the available depocentre, and the possibility of transporting sediments farther into the basin is hindered. The only possibility is to have smaller amount of sands transported to the slope. The strike elongation of shelf-edge deltas in this second model is associated with the abrupt increase in accommodation reflecting an increased influence of tectonic and sediment load induced subsidence rather than any particular hydraulic regime on the outer shelf. In the areas affected by precursor growth fault, the thickest part of the wedge (Fig. 21) tends to be located relatively landward of the physiography.

The third model (Fig. 25) combines the first and second models to create shelf-edge models for prediction of sand transportation and deposition when comparing two co-planar faults that are of different age. The model clearly shows evidence that in the presence of precursor growth fault with large depocentres, much sands will be deposited in its subsidence axis and there will be limited amount of sands to be transported farther in the basinward direction, while for the younger faults formed at a younger age, it would allow the possible transportation of large amount of sands from the shelf-edge to the basin floor. However, in situation of repeated wedges in the basinward direction of a sequence, there is a likelihood of having more sands accumulated at the proximal wedges as compared to the distal wedges.

## Conclusion

The dip adjusted semblance slices, growth fault indexes and seismic transect sections aided the interpretation of the growth fault dynamics and evolution. The point of origination of a fault or fracture failure initiation point is the point of most active growth in the fault system, and this is reflected in the vertical growth of sediments across the fault as the thickest sediment will be associated with this initiation point. Thus, as the fault propagates and grows over time, it tends to influence/initiate faulting activities around it and dominantly in the direction of propagation. Precursor older faults associated with large depocentres in the form of wedges have proven to provide accommodation space to massive sand deposits, while younger faults that were initiated by adjacent co-planar faults with no significant depocentre have shown to limit the deposition of sands on the
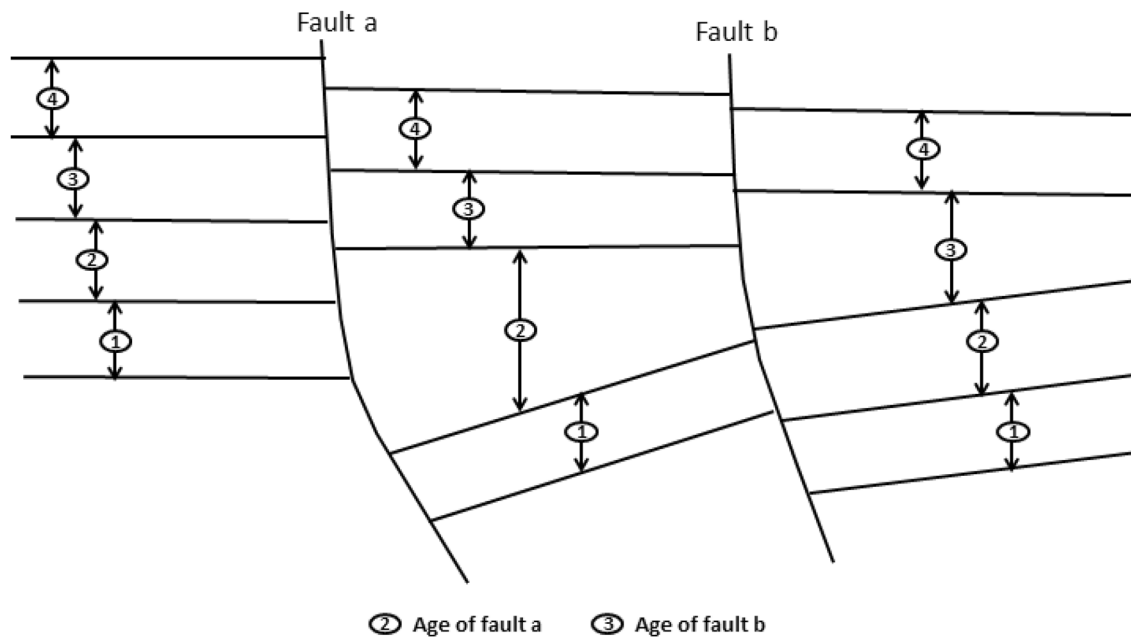
**Fig. 19** Concept of determination of relative ages of faults using major growth stratigraphic sequence

shelf-edge, thus allowing the deposition of sands farther into the basinward direction due to the underlying substratum.

This study has shown that faults do follow a systematic direction of propagation such that the direction at which a fault propagates (paleo-stress direction) is the likely direction of formation of more faults. Four gross depositional environments have been interpreted from this study (using combined evaluation of lithofacies and paleobathymetry): inner-shelf, middle-shelf, shelf-edge (shelf-margin) and slope environments. Large sand units have been recognized at the shelf-edge environment at the deeper and top parts of the sequence. The thickest sands towards the top of the sequence are of the lowstand system tracts, while the thinner sands below are of highstand system tracts. Generally, the shelf-edge delta has higher sand percentage than the slope. The geobody interpretation showed that sands associated with younger faults (geobody located towards the south and coloured in purple) as shown in Fig. 8 will be transported farther in the basinward direction, while sands associated with precursor older faults (geobody located towards the south and coloured in red) will permit massive sand deposits at the fault-related depocentres and limit the possibility of transporting more sands towards the basinward direction.

The integrated subsurface data interpretation and conceptual models in Figs. 20, 21 and 22 show that there is an increase in reservoir thickness and net to gross in the proximal part of the sequence associated with precursor older faults, while towards the distal part, it gradually reduces with sands thinning towards the base of the stratigraphic units in the form of pinch out. The strike elongation of the

shelf-edge delta on precursor fault is associated with the abrupt increase in the accommodation space. The accommodation space is increased further by gravity influence whose instability increases with an increased sediment supply. There is also a relative decrease in reservoir thickness and net to gross in the proximal part of the sequence associated with younger initiated fault, while towards the distal part, it gradually increases in reservoir thickness and net to gross. The dip elongation and increase in distal proportion of the sands associated with younger fault show that more sands will be transported to the basin floor within this regime.

In conclusion, this study has resulted into building of conceptual models which compares two co-planar growth faults within the shelf-edge and the associated possibility of sediment transportation from the shelf-edge to the basin floor (Figs. 23, 24, 25). It clearly shows that there are unique sedimentation patterns associated with the two faults, as the precursor fault (which started forming within sequence 31.3 to 33.0 MFS) is associated with bigger sand deposit close to the proximal part of the hanging-wall depocentre which limits the amount of sand that gets to the basin, while younger faults formed after deposition of sequence 31.3 to 33.0 MFS are associated with basinward increase in depocentre which allows more sand to be transported to the basin. This can serve as a prediction model for explorationists and researchers when searching for prospective hydrocarbon sands where a shelf-edge environment has been identified.
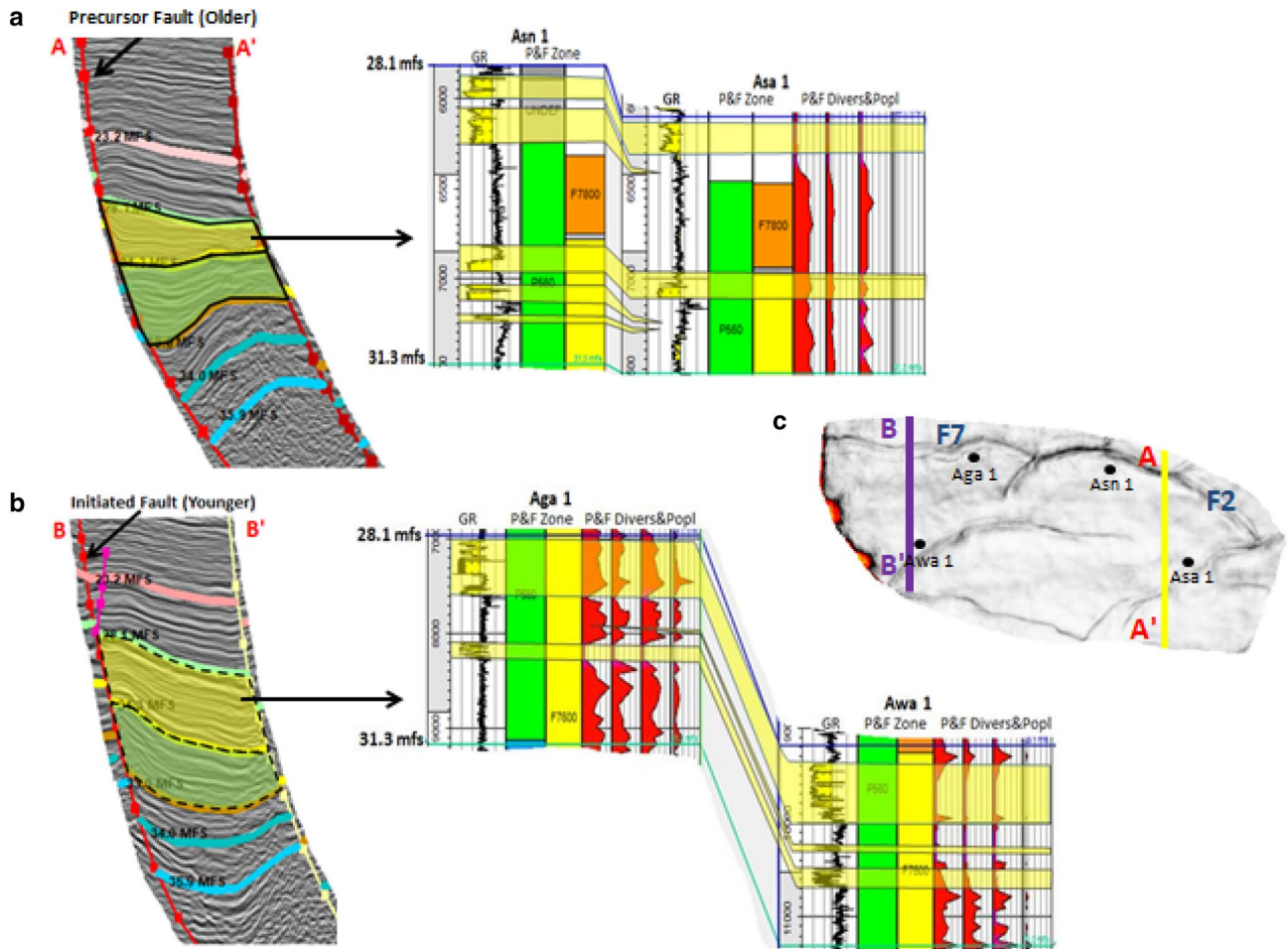
**Fig. 20** Seismic traverses and well logs correlation across **a** precursor fault 2 adjacent seismic reflection geometry and reservoir distribution, **b** initiated younger fault 7 adjacent seismic reflection geometry and reservoir distribution, **c** semblance slice showing the line of sections, of two co-planar faults (F2 and F7) and well locations
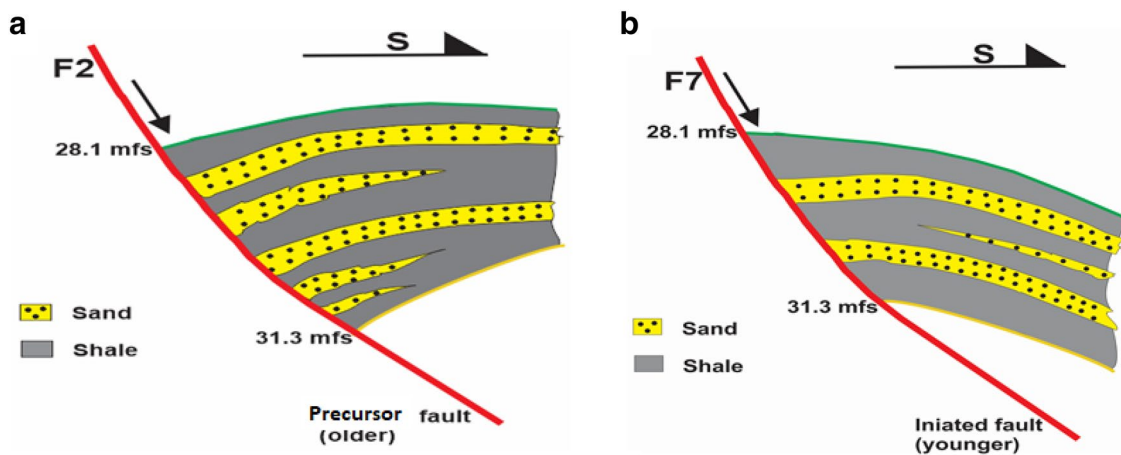


**Fig. 21** **a** Precursor fault and associated facies change within sequence 28.1 MFS to 31.3 MFS, **b** initiated younger fault and associated facies change within sequence 28.1 MFS to 31.3 MFS

**Fig. 22** Changes in net to gross and axis of subsidence arising from same sequence associated with precursor and younger co-planar faults
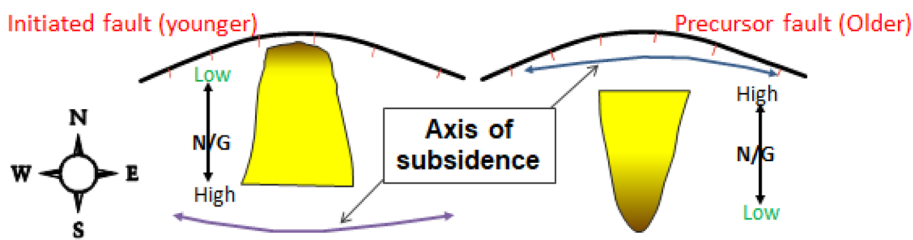


**Fig. 23** Tectono-depositional model of younger growth fault association with sand distribution and transportation from the shelf-edge to the basin floor
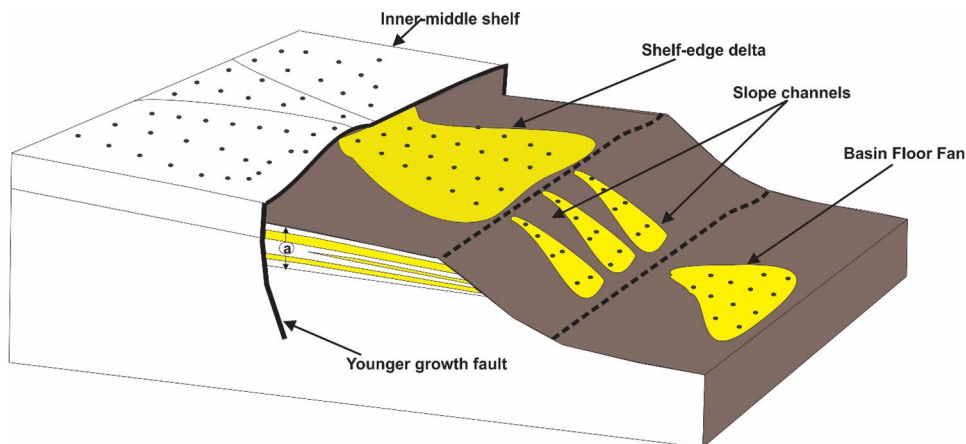


**Fig. 24** Tectono-depositional model of precursor older fault association with sand distribution and transportation from the shelf-edge to the slope
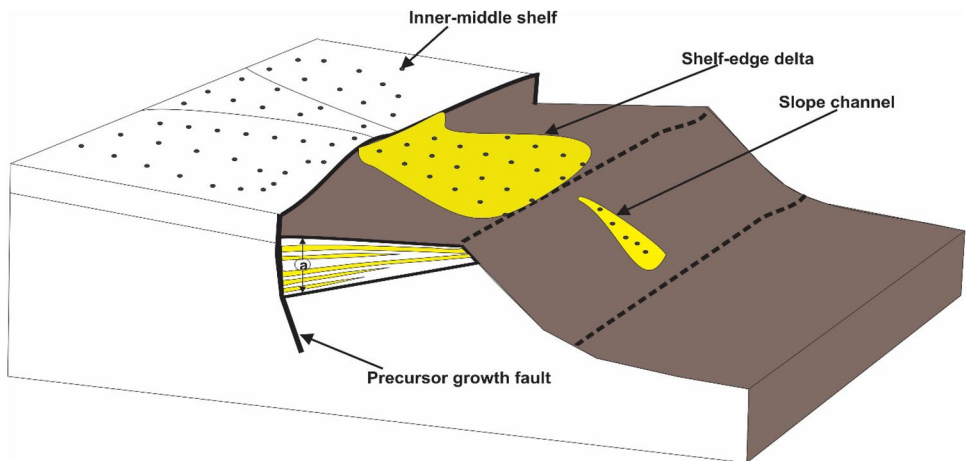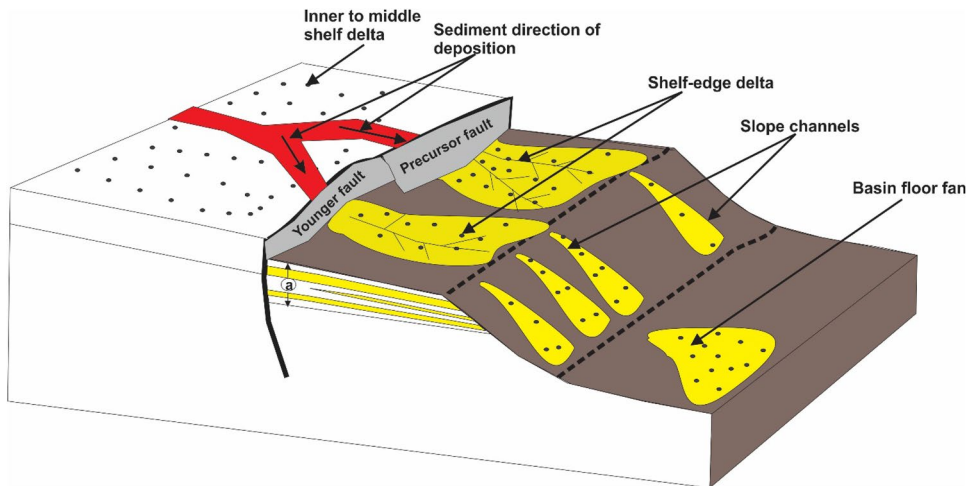


**Fig. 25** Tectono-depositional model of two co-planar growth faults and their association with sand distribution and transportation from the shelf-edge to the basin floor

## References

Adereti O, Feldman H, Unomah G et al (2012) Key elements of a world class petroleum system: lowstand shelf edge reservoirs in the Southeastern Niger Delta, Nigeria. NAPE Bull 24(1):38–42

Allen JRL (1965) Late Quaternary Niger Delta, and adjacent areas-sedimentary environments and lithofacies. AAPG Bull 49:547–600

Anomneze DO (2014) Proven and possible petroleum plays of the Eastern Niger Delta Basin, Nigeria. In: Proceedings of SPE Nigeria annual international conference and exhibition

Anomneze DO, Okoro AU, Ajaegwu NE, Akpunonu EO, Ahaneku CV, Ede TAD, Okeugo GC, Ejeke CF (2015) Application of seismic stratigraphy and structural analysis in the determination of petroleum plays within the eastern Niger Delta Basin, Nigeria. J Petrol Explor Prod Technol 5(2):113–122

Clayton CA, Anis M, Cooley TW, Troyer WH, Wallace JP, Cohen MF, Fadase AO, Pebdani FN, Odior EG, Ekworomadu EO, Nwaeri EU, Membere AH (1998) Integrated reservoir management, Ubit field, offshore Nigeria. AAPG Bull 82:1901–1909

Dixon JF, Steel RJ, Olariu C (2012) Shelf-edge delta regime as a predictor of deepwater deposition. J Sediment Res 82:681–687

Doglioni C, Dagostino N, Mariotti G (1998) Normal faulting vs regional subsidence and sedimentation rate. Mar Pet Geol 15(8):737–750

Doust HE, Omatsola EM (1989) Niger delta regression transgression cycles. AAPG Mem 48:201–238

Edwards MB (1981) Upper Wilcox Rosita delta system of south Texas: growth-faulted shelf-edge deltas. AAPG Bull 65:54–73

Ejedawe J, Love F, Steele D and Ladipo K (2007) Onshore to deepwater geologic integration, Niger Delta. An in-house presentation pack of the Shell Petroleum and Development Company, Port-Harcourt

Embry AF (2009) Practical sequence stratigraphy. CSPG Bull 5:50–70

Fieldman H, Adereti O, Ahmed B et al (2013) Predicting large-scale reservoir architecture: application of data from shelf edge reservoirs in the Eastern Niger Delta. NAPE Bull 25(1):52–60

Fossen H, Rotevatn A (2016) Fault linkage and relay structures in extensional settings—a review. Earth Sci Rev 154:14–28

Galloway WE (1989) Genetic stratigraphic sequences in basin analysis: architecture and genesis of flooding-surface bounded depositional units. AAPG Bull 73:125–142

Gibbs AD (1983) Balanced cross-section construction from seismic sections in areas of extensional tectonics. J Struct Geol 5(2):153–160

Khalil SM, McClay KR (2001) Extensional fault-related folding, northwestern Red Sea, Egypt. J Struct Geol 24:743–762

Mayall MJ, Yielding CA, Oldroyd JD, Pulham AJ, Sakurai S (1992) Facies in a shelf-edge delta—an example from the subsurface of the Gulf of Mexico, middle Pliocene, Mississippi Canyon, Block 109. AAPG Bull 76:435–448

Mellere D, Steel RJ (1995) Variability of lowstand wedges and their distinction from forced regressive wedges in the Mesaverde Group, southeast Wyoming. Geology 23:803–806

Mitchener BC, Lawrence DA, Partington MA, Bowman MBJ, Gluyas J (1992) Brent Group sequence stratigraphy and regional implications. Geol Soc Spec Publ 61:45–80

Morton RA, Suter JR (1996) Sequence stratigraphy and composition of Late Quaternary shelf-margin deltas, Northern Gulf of Mexico. AAPG Bull 80:505–530

Obiadi II, Obiadi CM (2016) Structural deformation and depositional processes: insights from the Greater Ughelli Depobelt, Niger Delta, Nigeria. Oil Gas Res 2(3):1–8

Ocamb R (1961) Growth faults of South Louisiana. Gulf Coast Assoc Geol Soc Bull 11:139–175

Oliveira MJ, Zalan PV, Caldeira JL, Tanaka A, Santarem P, Trosdtorf I, Moraes A (2012) Linked environment—compressional tectonics in gravitational systems in the Equatorial Margin of Brazil. AAPG Mem 100:159–178

Paumard V, Bourget J, Payenberg T, Ainsworth R, George A, Lang S, Posamentier H, Peyrot D (2018) Controls on shelf-margin architecture and sediment partitioning during a syn-rift to post-rift transition: insights from the Barrow Group (Northern Carnarvon Basin, North West Shelf, Australia). Earth Sci Rev 177:643–677

Plink-Bjorklund P, Mellere D, Steel RJ (2001) Turbidite variability and architecture of sand-prone, deepwater slopes: Eocene clinoforms in the Central Basin, Spitsbergen. J Sediment Res 71:897–914

Porebski SJ, Steel RJ (2001) Delta types and sea level cycle. In: Proceedings from AAPG annual convention, Denver, Colorado, vol 10, pp 160–170

Porebski SJ, Steel RJ (2003) Shelf-margin deltas: their stratigraphic significance and relation to deepwater sands. Earth Sci Rev 62:283–326

Posamentier HW, Allen GP, James DP, Tesson M (1992) Forced regressions in a sequence stratigraphic framework: concepts, examples and exploration significance. AAPG Bull 76:1687–1709

Prather BE, Booth JR, Steffens GS, Craig PA (1998) Classification, lithologic calibration, and stratigraphic succession of seismic facies of intraslope basins, deep-water Gulf of Mexico. AAPG Bull 82:701–728

Steel RJ, Crabaugh J, Schellpeper M, Mellere D, Plink-Bjorklund P, Deibert J, Loeseth T (2000) Deltas versus rivers on the shelf edge: their relative contributions to the growth of shelf margins and basin-floor fans (Barremian and Eocene, Spitsbergen). In: Proceedings GCSSEPM foundation 20th annual research conference, deepwater reservoirs of the world, Houston, pp 981–1000

Suter JR, Berryhill HL (1985) Late quaternary shelf-margin deltas, northwest Gulf of Mexico. AAPG Bull 69:77–91

Sydow J, Roberts HH (1994) Stratigraphic framework of a Late Pleistocene shelf-edge delta, Northeast Gulf of Mexico. AAPG Bull 78:1276–1312

Wood LJ, Hentz T, Zeng H, DeAngelo M, Dutton S (2003) Applying sequence stratigraphy and seismic stratal slice technology in the Gulf of Mexico. In: Proceedings of gas tips conference, pp 10–15

Xue L, Galloway WL (1995) High-resolution depositional framework of the Paleocene middle Wilcox strata, Texas coastal plain. AAPG Bull 79:205–230